Noname manuscript No.
(will be inserted by the editor)

Weakly nonlinear analysis of two dimensional sheared granular flow

Kuniyasu Saitoh · Hisao Hayakawa

Received: date / Accepted: date

Abstract Weakly nonlinear analysis of a two dimensional sheared granular flow is carried out under the Lees-Edwards boundary condition. We derive the time dependent Ginzburg-Landau (TDGL) equation of a disturbance amplitude starting from a set of granular hydrodynamic equations and discuss the bifurcation of the steady amplitude in the hydrodynamic limit.

Keywords Sheared granular flow · Reduction theory · the Ginzburg-Landau equation

1 Introduction

To control flows of granular particles is important in science and industry [1,2,3,4,5]. However, the properties of granular flow have not been well understood yet, because they behave as unusual fluids [6]. This unusual nature is mainly caused by inelastic collisions between granular particles. Indeed, there is no equilibrium state in granular materials because of the inelastic collisions, which suggests that granular materials are an appropriate target of nonequilibrium statistical mechanics [7].

Although there are many studies of granular flows on inclined planes [5,8], the existence of gravity and the role of bottom boundary make the problem complicated. On the other hand, the granular flow under a plane shear is the simplest and an appropriate situation for theoretical analysis. Granular flows under the plane shear have been studied from many aspects such as the application of kinetic theory[9,10], shear band formation in moderate dense granular systems [11,12], long-time tail and long-range correlation function [13,14,15,16,17,18,19,20,21], pattern formation of dense flow [22, 23,24,25,26,27], determination of constitutive equation for dense flow [28,29,30], as

Kuniyasu Saitoh
Yukawa Institute for Theoretical Physics, Kyoto University, Sakyoku, Kyoto 606-8502, Japan
Tel.: +81-075-753-7063
E-mail: saitoh@yukawa.kyoto-u.ac.jp

Hisao Hayakawa
Yukawa Institute for Theoretical Physics, Kyoto University, Sakyoku, Kyoto 606-8502, Japan
E-mail: hisao@yukawa.kyoto-u.ac.jp

well as jamming transition [31,32,33,34,35,36]. In this paper, we focus on the formation of shear bands for moderate dense granular gases observed in the discrete element method (DEM) simulations [11,12]. When we adopt a physical boundary condition, two shear bands are formed near the boundary in the early stage, and move to form the one shear band in the center region. A similar shear band formation can be observed even under the Lees-Edwards boundary condition. The dynamic behavior of the shear band formation is reproduced by a simulation of granular hydrodynamic equations [12] derived from the kinetic theory for granular gases [3,37,38,39,40,41,42,43,44]. In addition, the linear stability analyses suggest that a homogeneous state of the sheared granular flow is almost always unstable [45,46,47].

Amongst many papers, it is notable that Khain found the coexistence of a solid phase and a liquid phase of granular particles from a molecular dynamics simulation for a dense sheared granular flow [26,27]. From the control of the value of the restitution coefficient, he demonstrated the existence of a hysteresis loop of the density difference between the boundary layer and the center region of the container. Employing a set of the hydrodynamic equations, he explained the mechanism to appear a subcritical bifurcation. This subcritical bifurcation seems to be different from that observed in the jamming transition of frictional particles [48].

Recently, Shukla and Alam carried out a weakly nonlinear analysis of a plane sheared granular flow [49,50], where they derived the Stuart-Landau equation of disturbance amplitude [51,52] starting from a set of granular hydrodynamic equations. They found a subcritical bifurcation in relatively dilute systems and the supercritical bifurcation in other parameter space. In their work, they assumed that the disturbances of the hydrodynamic fields do not depend on the mean flow direction under a mixed boundary condition, in which the base state satisfies the different boundary condition from that for the disturbance field. However, the slow process such as the merging of the shear bands was not discussed, because they adopt the method by Reynolds and Potter [53] which does not include any spatial degree of freedom. We also indicate that their perturbation is based on the analysis for a finite size system, in which the relation between the perturbation parameter and shear rate becomes unclear. To clarify the argument, we focus on the hydrodynamic limit case.

In this paper, we derive the time dependent Ginzburg-Landau (TDGL) equation as an amplitude equation of the disturbance field [54,55,56,57] starting from a set of granular hydrodynamic equations [43]. In our analysis, we take into account the dependence on the mean flow direction and adopt the Lees-Edwards boundary condition [58] to avoid difficulties caused by the physical boundary conditions. We discuss the bifurcation in the hydrodynamic limit from the results of the coefficients of the TDGL equation. We organize this paper as follows: In Sec.2, we explain the geometrical setup and basic equations of a two dimensional sheared granular flow. In Sec.3, we carry out the linear stability analysis. Section 4 is the main part of this paper, in which we derive the TDGL equation with the aid of the weakly nonlinear analysis. Finally, we discuss our analysis and describe our conclusion in Sec.5.

2 Setup and basic equations

Let us introduce our setup and basic equations. To avoid difficulties caused by the physical boundary conditions, we use the Lees-Edwards boundary condition, in which the upper and lower image cells move to the opposite direction with the speed $U/2$

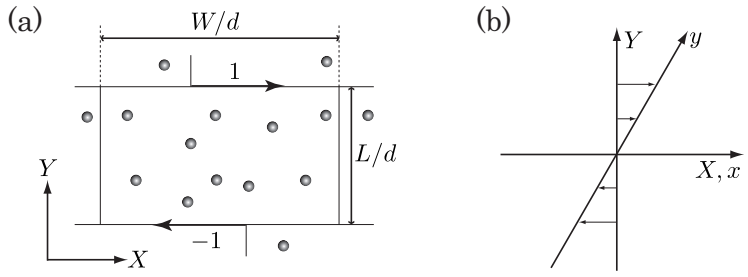

Fig. 1 (a) Geometrical setup of the two dimensional sheared granular flow under the Lees-Edwards boundary condition. The upper and lower image cells move to the opposite direction with the dimensionless speed 1. The dimensionless width and height of each cell are W/d and L/d, respectively. (b) A schematic relationship among X, Y, x and y axes.

[58]. The geometry of our setup is illustrated in Fig.1(a), where we adopt the diameter of a granular disk d and $U/2$ for the unit of length and speed, respectively. Therefore, if we define $\epsilon \equiv \sqrt{2d/L}$, the dimensionless *shear rate* is ϵ^2. In the following, we also use the mass of a granular disk m and $2d/U$ as the unit of mass and time, respectively.

We employ a set of hydrodynamic equations derived from the kinetic theory of granular gases [43]. Although the angular momentum and the spin temperature are included in the hydrodynamic equations, we ignore such rotational degrees of freedom to simplify our analysis. This simplification can be justified if the friction constant is small, because the effect of the tangential restitution coefficient and the rotation of particles during the collision can be absorbed in the normal restitution coefficient [59, 60].

We present the derivation of the following set of dimensionless hydrodynamic equations in Appendix A:

$$(\partial_T + \mathbf{v}\cdot\nabla)\,\nu = -\nu\nabla\cdot\mathbf{v} \tag{1}$$

$$\nu\,(\partial_T + \mathbf{v}\cdot\nabla)\,\mathbf{v} = -\nabla\cdot\mathbf{P} \tag{2}$$

$$(\nu/2)\,(\partial_T + \mathbf{v}\cdot\nabla)\,\theta = -\mathbf{P}:\nabla\mathbf{v} - \nabla\cdot\mathbf{q} - \chi\ , \tag{3}$$

where ν, $\mathbf{v}$, θ, T and $\nabla = (\partial/\partial_X, \partial/\partial_Y)$ are the area fraction, the dimensionless velocity field, the dimensionless granular temperature, the dimensionless time and the dimensionless gradient, respectively. The pressure tensor $\mathbf{P}$, the heat flux $\mathbf{q}$ and the energy dissipation rate χ are given by

$$\mathbf{P} = \left[p^*(\nu)\theta - \xi^*(\nu)\theta^{1/2}\,(\nabla\cdot\mathbf{v})\right]\delta_{ij} - \eta^*(\nu)\theta^{1/2}D'_{ij}\ , \tag{4}$$

$$\mathbf{q} = -\kappa^*(\nu)\theta^{1/2}\nabla\theta - \lambda^*(\nu)\theta^{3/2}\nabla\nu\ , \tag{5}$$

$$\chi = \frac{1-e^2}{4\sqrt{2\pi}}\nu^2 g(\nu)\theta^{1/2}\left[4\theta - 3\sqrt{\frac{\pi}{2}}\theta^{1/2}\,(\nabla\cdot\mathbf{v})\right]\ , \tag{6}$$

respectively. Here, D'_{ij} $(i,j = X,Y)$ is the deviatoric part of the strain rate

$$D'_{ij} \equiv \frac{1}{2}\left(\nabla_j v_i + \nabla_i v_j - \delta_{ij}\nabla\cdot\mathbf{v}\right)\ , \tag{7}$$

and $p^*(\nu)\theta$, $\xi^*(\nu)\theta^{1/2}$, $\eta^*(\nu)\theta^{1/2}$, $\kappa^*(\nu)\theta^{1/2}$ and $\lambda^*(\nu)\theta^{3/2}$ are the static pressure, the bulk viscosity, the shear viscosity, the heat conductivity and the coefficient associated

Table 1 The functions in Eqs.(4)-(6), where e is the restitution coefficient.

$p^*(\nu)$	=	$\frac{1}{2}\nu\left[1+(1+e)\nu g(\nu)\right]$
$\xi^*(\nu)$	=	$\frac{1}{\sqrt{2\pi}}(1+e)\nu^2 g(\nu)$
$\eta^*(\nu)$	=	$\sqrt{\frac{\pi}{2}}\left[\frac{g(\nu)^{-1}}{7-3e}+\frac{(1+e)(3e+1)}{4(7-3e)}\nu+\left(\frac{(1+e)(3e-1)}{8(7-3e)}+\frac{1}{\pi}\right)(1+e)\nu^2 g(\nu)\right]$
$\kappa^*(\nu)$	=	$\sqrt{2\pi}\left[\frac{g(\nu)^{-1}}{(1+e)(19-15e)}+\frac{3(2e^2+e+1)}{8(19-15e)}\nu+\left(\frac{9(1+e)(2e-1)}{32(19-15e)}+\frac{1}{4\pi}\right)(1+e)\nu^2 g(\nu)\right]$
$\lambda^*(\nu)$	=	$-\sqrt{\frac{\pi}{2}}\frac{3e(1-e)}{16(19-15e)}\left[4(\nu g(\nu))^{-1}+3(1+e)\right]\frac{d\left(\nu^2 g(\nu)\right)}{d\nu}$

with the gradient of density, respectively. The explicit forms of them are listed in Table 1, where we adopt

$$g(\nu)=\frac{1-7\nu/16}{(1-\nu)^2} \tag{8}$$

for the radial distribution function at contact which is only valid for $\nu<0.7$ [61,62, 63,64]. It should be noted that the expression of $\kappa(\nu)$ in Ref.[12] contains an error (see Appendix A).

3 Linear stability analysis

In this section, we present the linear stability analysis of a sheared granular flow under the Lees-Edwards boundary condition. Although the analysis is essentially the same with the previous studies [45,46,47], it is necessary as the basis of the weakly nonlinear analysis.

3.1 Stretched coordinate

We introduce a stretched coordinate (x,y) as illustrated in Fig.1(b), where the origin is common with that of a Cartesian coordinate (X,Y) [65,66,67]. The mutual relationships with (X,Y) and T are given by

$$\begin{cases} x=X-\epsilon^2 TY \\ y=Y \\ t=T \end{cases}, \tag{9}$$

where t is the time in the stretched coordinate. Thus, the differential operators are transformed as [65,66,67]

$$\begin{cases} \partial_X=\partial_x \\ \partial_Y=\partial_y-\epsilon^2 t\partial_x \\ \partial_T=\partial_t-\epsilon^2 y\partial_x \end{cases}. \tag{10}$$

3.2 Eigenvalue problem

Because the y axis changes together with the mean stream $\mathbf{v}_0 = (\epsilon^2 Y, 0)$, the velocity field in the stretched coordinate is given by $(u, w) = \mathbf{v} - \mathbf{v}_0$. If we denote the hydrodynamic field in the stretched coordinate as $\phi \equiv (\nu, u, w, \theta)^{\mathrm{T}}$, where the superscript T represents the transposition, the material derivative is transformed as

$$\begin{aligned}\partial_T \phi + \mathbf{v}\cdot\nabla\phi &= \partial_t\phi - \epsilon^2 y\partial_x\phi + \epsilon^2 y\partial_x\phi + u\partial_x\phi + w\partial_y\phi \\ &= \partial_t\phi + u\partial_x\phi + w\partial_y\phi \ . \end{aligned} \tag{11}$$

Thus the convective term $\epsilon^2 y\partial_x\phi$ can be eliminated for later discussion. A set of homogeneous solutions of Eqs.(1)-(3) is given by $\phi_0 \equiv (\nu_0, 0, 0, \theta_0)^{\mathrm{T}}$, where ν_0 is the mean area fraction and

$$\theta_0 = \sqrt{\frac{\pi}{2}}\frac{\epsilon^4\eta^*(\nu_0)}{(1-e^2)\,\nu_0^2 g(\nu_0)} \tag{12}$$

is the mean granular temperature.

We introduce the disturbance field $\hat{\phi}(x, y, t) \equiv \phi - \phi_0$ which can be expanded by a plane wave as

$$\hat{\phi}(x, y, t) = \sum_{\mathbf{k}(t)} A\phi_{\mathbf{k}(t)} e^{i\mathbf{k}(t)\cdot\mathbf{x}} e^{\sigma t} \tag{13}$$

under the Lees-Edwards boundary condition, where σ is a complex number, A is an amplitude and $\mathbf{x} = (x, y)$. The dimensionless wave number vector in the stretched coordinate is given by $\mathbf{k}(t) \equiv (k_x, k_y(t)) \equiv (K_X, K_Y + \epsilon^2 t K_X)$, where (K_X, K_Y) is the dimensionless wave number vector in the Cartesian coordinate. Because we assume that the hydrodynamic field satisfies the symmetry

$$\begin{pmatrix} \nu(-x,-y,t) \\ u(-x,-y,t) \\ w(-x,-y,t) \\ \theta(-x,-y,t) \end{pmatrix} = \begin{pmatrix} \nu(x,y,t) \\ -u(x,y,t) \\ -w(x,y,t) \\ \theta(x,y,t) \end{pmatrix} \ , \tag{14}$$

which is usually observed in numerical simulations [12], we adopt

$$\phi_{\mathbf{k}(t)} = (\nu_{\mathbf{k}(t)}, iu_{\mathbf{k}(t)}, iw_{\mathbf{k}(t)}, \theta_{\mathbf{k}(t)})^{\mathrm{T}} \ , \tag{15}$$

where $\nu_{\mathbf{k}(t)}, u_{\mathbf{k}(t)}, w_{\mathbf{k}(t)}$ and $\theta_{\mathbf{k}(t)}$ are real functions of $\mathbf{k}(t)$.

If we linearize Eqs.(1)-(3) by $\hat{\phi}(x, y, t)$ with taking into account Eqs.(10), (11) and (13), the problem is reduced to solving an eigenvalue problem

$$\mathcal{L}\varphi_{\mathbf{k}(t)} = \sigma\varphi_{\mathbf{k}(t)} \ , \tag{16}$$

where we defined a real eigenvector $\varphi_{\mathbf{k}(t)} \equiv (\nu_{\mathbf{k}(t)}, u_{\mathbf{k}(t)}, w_{\mathbf{k}(t)}, \theta_{\mathbf{k}(t)})^{\mathrm{T}}$ and the 4×4 real matrix

$$\mathcal{L} = \begin{pmatrix} 0 & \nu_0 k_x & \nu_0 k_s(t) & 0 \\ \epsilon^2\frac{\eta_0'}{2}k_s(t) - p_0' k_x & -\xi_0 k_x^2 - \frac{\eta_0}{2}\mathbf{s}(t)^2 & -\xi_0 k_x k_s(t) - \epsilon^2 & \epsilon^2\frac{\eta_0}{4\theta_0}k_s(t) - \frac{p_0}{\theta_0}k_x \\ \epsilon^2\frac{\eta_0'}{2}k_x - p_0' k_s(t) & -\xi_0 k_x k_s(t) & -\xi_0 k_s(t)^2 - \frac{\eta_0}{2}\mathbf{s}(t)^2 & \epsilon^2\frac{\eta_0}{4\theta_0}k_x - \frac{p_0}{\theta_0}k_s(t) \\ C_1 - 2\lambda_0\mathbf{s}(t)^2 & -2\epsilon^2\eta_0 k_s(t) - C_2 k_x & -2\epsilon^2\eta_0 k_x - C_2 k_s(t) & C_3 - 2\kappa_0\mathbf{s}(t)^2 \end{pmatrix} \tag{17}$$

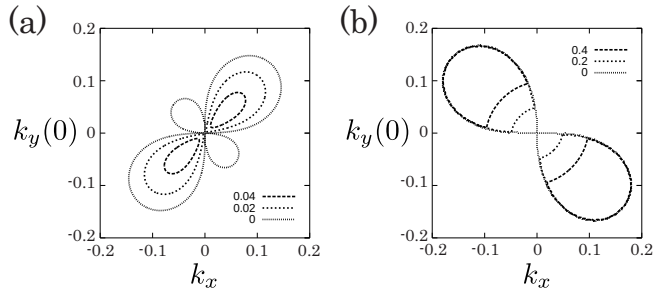

Fig. 2 Contour plots of (a) Re[σ] and (b) Im[σ] at $t = 0$. Re[σ] and Im[σ] are negative outside the contour line. Here, we have used $\epsilon = 0.01$, $e = 0.992$ and $\nu_0 = 0.3$.

with $\mathbf{s}(t) \equiv (k_x, k_s(t)) \equiv (k_x, k_y(t) - \epsilon^2 t k_x)$, and

$$C_1 = \epsilon^4 \eta_1 - \sqrt{\frac{2}{\pi}} \left(1 - e^2\right) (g_0 + \nu_0 g_1) \, \theta_0^{3/2} \ , \tag{18}$$

$$C_2 = \frac{3}{4} \left(1 - e^2\right) \nu_0 g_0 \theta_0 - 2 p_0 \ , \tag{19}$$

$$C_3 = \frac{\epsilon^4 \eta_0}{2\theta_0} - \frac{3}{\sqrt{2\pi}} \left(1 - e^2\right) \nu_0 g_0 \theta_0^{1/2} \ . \tag{20}$$

The coefficients of the Taylor expansion, i.e. g_0, g_1, p_0, p_0', etc. are given in Appendix B.

Figure 2 displays (a) the real and (b) imaginary parts of σ at $t = 0$. Figure 3 shows the time evolution of the real part of σ. Here, we use $\epsilon = 0.01$, $e = 0.992$ and $\nu_0 = 0.3$, and numerically solve the eigenvalue problem Eq.(16) by LAPACK [68]. Although the unstable region is stretched to the $k_y(t)$ direction as time evolves, the maximum value of Re[σ] always exists in the direction of the unit vector

$$\mathbf{n}(t) = \frac{1}{\sqrt{1 + (1 + \epsilon^2 t)^2}} (1, 1 + \epsilon^2 t) \ , \tag{21}$$

which is illustrated as an arrow in Fig.3(c).

3.3 Hydrodynamic limit

If $\epsilon = 0$, the growth rate is neutral, i.e. $\sigma_c = 0$, at the neutral mode $\mathbf{k}_c(t) = \mathbf{0}$ with the critical restitution coefficient $e_c = 1$. Thus, in the hydrodynamic limit $\epsilon \ll 1$ with the fixed mean temperature θ_0, it is found from Eq.(12) that $1 - e^2$ is scaled as $1 - e^2 = \epsilon^4$.

Because the maximum value of Re[σ] for $\epsilon > 0$ exists in the direction $\mathbf{n}(t)$, we scale the wave number as

$$\mathbf{k}(\tau) = \epsilon q (1, 1 + \tau) \ , \tag{22}$$

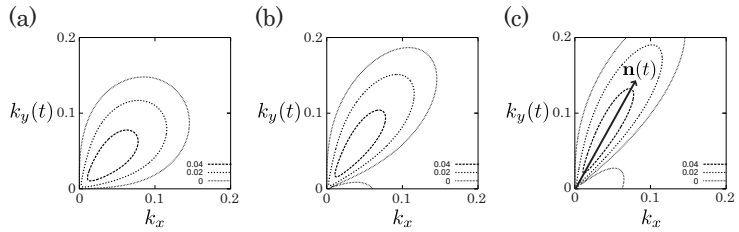

Fig. 3 Contour plot of Re[σ] at (a) $t = 0$, (b) $t = 6.5d/U$ and (c) $t = 13d/U$, respectively. $\mathbf{n}(t)$ is illustrated as an arrow in (c).

where we have introduced a long time scale $\tau \equiv \epsilon^2 t$ and a scaled wave number q. Because $k_s(t)$ and $\mathbf{s}(t)$ respectively satisfy $k_s(t) = \epsilon q$ and $\mathbf{s}(t) = \epsilon q(1,1)$, Eq.(16) is reduced to

$$\mathcal{L}_q \varphi_q = \sigma(q)\varphi_q \ , \tag{23}$$

where $\mathcal{L}_q$ is given by

$$\mathcal{L}_q = \begin{pmatrix} 0 & \epsilon q\nu_0 & \epsilon q\nu_0 & 0 \\ \epsilon^3 q\frac{\eta_0'}{2} - \epsilon q p_0' & -\epsilon^2 q^2(\xi_0+\eta_0) & -\epsilon^2 q^2\xi_0 - \epsilon^2 & \epsilon^3 q\frac{\eta_0}{4\theta_0} - \epsilon q\frac{p_0}{\theta_0} \\ \epsilon^3 q\frac{\eta_0'}{2} - \epsilon q p_0' & -\epsilon^2 q^2\xi_0 & -\epsilon^2 q^2(\xi_0+\eta_0) & \epsilon^3 q\frac{\eta_0}{4\theta_0} - \epsilon q\frac{p_0}{\theta_0} \\ C_1 - 4\epsilon^2 q^2\lambda_0 & -2\epsilon^3 q\eta_0 - \epsilon q C_2 & -2\epsilon^3 q\eta_0 - \epsilon q C_2 & C_3 - 4\epsilon^2 q^2\kappa_0 \end{pmatrix} . \tag{24}$$

We stress that $\mathcal{L}_q$ does not depend on time. As a result, the eigenvalue $\sigma(q)$ and the eigenvector φ_q are also independent of time.

Now, we carry out the perturbative calculation of the eigenvalue problem Eq.(23) (see Appendix C) and the dispersion relation is given by

$$\sigma(q) = \epsilon^2\left(\frac{1}{2} - \epsilon^2 c\right) - \eta_0\epsilon^2 q^2 - \frac{\epsilon^4\theta_0}{16J^2q^2} - \frac{\epsilon^4 a}{bJ^2(bq^2 - J^2)} \ , \tag{25}$$

where $\sigma(q)$ is a real function of q and truncated at $O(\epsilon^4)$. The real constants J, a, b and c are given by Eqs.(118), (160)-(162) in Appendix C, respectively.

The prefactor $q_{\rm m}$, which gives the maximum value of $\sigma(q)$, is given by $d\sigma(q)/dq = 0$. For $\epsilon \ll 1$, $q_{\rm m}$ satisfies

$$q_{\rm m} = q_0\epsilon^{1/2} + O(\epsilon^{5/2}) \ , \tag{26}$$

where $q_0 = (\theta_0/16\eta_0 J^2)^{1/4}$. Therefore, the most unstable mode is defined as

$$\mathbf{k}_{\rm m}(\tau) = \epsilon^{3/2} q_0(1, 1+\tau) \ . \tag{27}$$

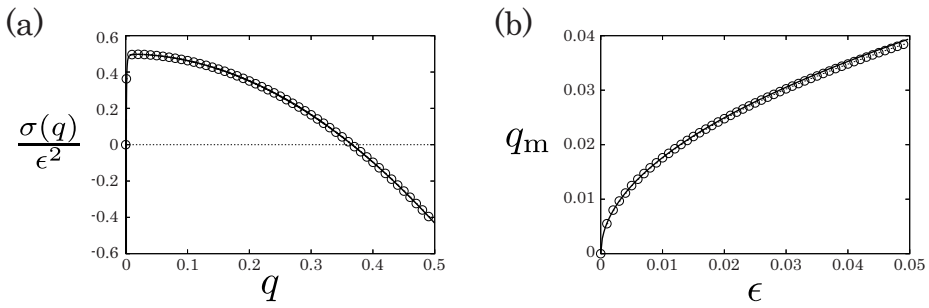

Fig. 4 (a) $\sigma(q)/\epsilon^2$ given by Eq.(25) and numerical result. The solid line and the open circles represent Eq.(25) and numerical result, respectively. (b) $q_{\rm m} = q_0\epsilon^{1/2}$ and numerical result of $q_{\rm m}$ as a function of ϵ. The solid line and the open circles represent $q_{\rm m} = q_0\epsilon^{1/2}$ and numerical result, respectively. Here, we use $\epsilon = 0.01$ and $\nu_0 = 0.3$.

From Eqs.(155) and (156) in Appendix C, the right and left eigenvectors of the most unstable mode are given by

$$\varphi_{q_{\rm m}} = \begin{pmatrix} \nu_{q_0} \\ u_{q_0} \\ w_{q_0} \\ \theta_{q_0} \end{pmatrix} = \begin{pmatrix} 0 \\ \frac{1}{\sqrt{2}} \\ -\frac{1}{\sqrt{2}} \\ 0 \end{pmatrix} + \epsilon^{1/2} \begin{pmatrix} \frac{\nu_0\theta_0}{2\sqrt{2}q_0J^2} \\ 0 \\ 0 \\ \frac{\theta_0 p_0}{\sqrt{2}q_0J^2} \end{pmatrix} + \epsilon \begin{pmatrix} 0 \\ \frac{\theta_0}{8\sqrt{2}q_0^2J^2} \\ \frac{\theta_0}{8\sqrt{2}q_0^2J^2} \\ 0 \end{pmatrix} , \tag{28}$$

$$\tilde{\varphi}_{q_{\rm m}} = \begin{pmatrix} \tilde{\nu}_{q_0} \\ \tilde{u}_{q_0} \\ \tilde{w}_{q_0} \\ \tilde{\theta}_{q_0} \end{pmatrix} = \begin{pmatrix} 0 \\ \frac{1}{\sqrt{2}} \\ -\frac{1}{\sqrt{2}} \\ 0 \end{pmatrix} + \epsilon^{1/2} \begin{pmatrix} \frac{\theta_0 p_0'}{2\sqrt{2}q_0J^2} \\ 0 \\ 0 \\ \frac{p_0}{2\sqrt{2}q_0J^2} \end{pmatrix} + \epsilon \begin{pmatrix} 0 \\ -\frac{\theta_0}{8\sqrt{2}q_0^2J^2} \\ -\frac{\theta_0}{8\sqrt{2}q_0^2J^2} \\ 0 \end{pmatrix} , \tag{29}$$

respectively, where we truncated $\varphi_{q_{\rm m}}$ and $\tilde{\varphi}_{q_{\rm m}}$ at $O(\epsilon)$.

Figure 4(a) shows $\sigma(q)/\epsilon^2$ given by Eq.(25) and numerical result. Figure 4(b) displays $q_{\rm m} = q_0\epsilon^{1/2}$ and numerical result of $q_{\rm m}$ as a function of ϵ. In numerical calculations, we solve Eq.(23) by LAPACK [68]. Although the third term of Eq.(25) diverges at $q = 0$, Eq.(25) well reproduces the numerical result around $q_{\rm m}$ and larger value of q.

4 Weakly nonlinear analysis

This section is the main part of this paper, where we develop weakly nonlinear analysis and derive the TDGL equation.

4.1 Expansion of the disturbance field

To develop a weakly nonlinear analysis, we introduce a long time scale and long length scales as $\tau = \epsilon^2 t$ and $(\xi, \zeta) = \epsilon(x, y)$, respectively. Thus, the derivatives are scaled as

$$\nabla = \epsilon(\partial_\xi, \partial_\zeta), \qquad \partial_t = \epsilon^2\partial_\tau \ . \tag{30}$$

We expand the disturbance field $\hat{\phi}$ into the harmonics of the most unstable mode $\mathbf{k}_{\rm m}(\tau)$ and expand the amplitude of $\hat{\phi}$ into the series of ϵ as

$$\hat{\phi} = \left\{ \epsilon A_1(\xi,\zeta,\tau) + \epsilon^2 A_2(\xi,\zeta,\tau) + \epsilon^3 A_3(\xi,\zeta,\tau) + \dots \right\} \phi_{q_{\rm m}} e^{i\mathbf{q}_{\rm m}(\tau)\cdot\mathbf{z}} + (\text{higher harmonics}) + \text{c.c.}\ , \tag{31}$$

where $\mathbf{q}_{\rm m}(\tau) = \epsilon^{1/2} q_0 (1, 1+\tau)$, $\mathbf{z} = (\xi, \zeta)$, $\phi_{q_{\rm m}} = (\nu_{q_0}, i u_{q_0}, i w_{q_0}, \theta_{q_0})^{\rm T}$ and c.c. represents the *complex conjugate*. Substituting Eq.(31) into the hydrodynamic equations Eqs.(1)-(3) and collecting the order of ϵ, the 4×4 real matrix $\mathcal{L}_{q_{\rm m}}$ is expanded as

$$\mathcal{L}_{q_{\rm m}} = \epsilon^{3/2} \mathcal{M}_{3/2} + \epsilon^2 \mathcal{M}_2 + \dots\ , \tag{32}$$

where

$$\mathcal{M}_{3/2} = q_0 \begin{pmatrix} 0 & \nu_0 & \nu_0 & 0 \\ -p_0' & 0 & 0 & -p_0/\theta_0 \\ -p_0' & 0 & 0 & -p_0/\theta_0 \\ 0 & 2p_0 & 2p_0 & 0 \end{pmatrix}\ , \qquad \mathcal{M}_2 = \begin{pmatrix} 0 & 0 & 0 & 0 \\ 0 & 0 & -1 & 0 \\ 0 & 0 & 0 & 0 \\ 0 & 0 & 0 & 0 \end{pmatrix}\ . \tag{33}$$

4.2 The TDGL equation at $O(\epsilon^3)$

At $O(\epsilon^{5/2})$, we find

$$\mathcal{M}_{3/2} \varphi_{q_0} A_1 = 0 \tag{34}$$

and Eq.(28) satisfies Eq.(34) at this order of ϵ.

The first nonzero terms are found at $O(\epsilon^3)$, where the coefficient of $e^{i\mathbf{q}_{\rm m}(\tau)\cdot\mathbf{z}}$ satisfies

$$\varphi_{q_0} \partial_\tau A_1 = \mathcal{M}_2 \varphi_{q_0} A_1 + \mathcal{D}_1 \partial_\xi^2 A_1 + \mathcal{D}_2 \partial_\xi \partial_\mu A_1 + \mathcal{D}_3 \partial_\mu^2 A_1 + \mathcal{N}_3 A_1 |A_1|^2\ , \tag{35}$$

where we defined $\partial_\mu \equiv \partial_\zeta - \tau \partial_\xi$ and the real vectors $\mathcal{D}_1$, $\mathcal{D}_2$, $\mathcal{D}_3$ and $\mathcal{N}_3$ are given by

$$\mathcal{D}_1 = \begin{pmatrix} 0 \\ (\xi_0 + \eta_0/2) u_{q_0} \\ \eta_0 w_{q_0}/2 \\ 2\kappa_0 \theta_{q_0} \end{pmatrix}, \qquad \mathcal{D}_2 = \begin{pmatrix} 0 \\ \xi_0 w_{q_0} \\ \xi_0 u_{q_0} \\ 0 \end{pmatrix}, \qquad \mathcal{D}_3 = \begin{pmatrix} 0 \\ \eta_0 u_{q_0}/2 \\ (\xi_0 + \eta_0/2) w_{q_0} \\ 2\kappa_0 \theta_{q_0} \end{pmatrix}, \tag{36}$$

$$\mathcal{N}_3 = \begin{pmatrix} 0 \\ -p_2' \nu_{q_0}^3 - (p_1' + p_2) \nu_{q_0}^2 \theta_{q_0}/\theta_0 \\ -p_2' \nu_{q_0}^3 - (p_1' + p_2) \nu_{q_0}^2 \theta_{q_0}/\theta_0 \\ 2\nu_{q_0}(u_{q_0} + w_{q_0})(p_1 \theta_{q_0}/\theta_0 + p_2 \nu_{q_0}) \end{pmatrix}\ , \tag{37}$$

respectively. If we multiply $\tilde{\varphi}_{q_0}^{\rm T}$ to Eq.(35), we reach the time dependent Ginzburg-Landau (TDGL) equation of A_1 as

$$\partial_\tau A_1 = \alpha A_1 + d_1 \partial_\xi^2 A_1 + d_2 \partial_\xi \partial_\mu A_1 + d_3 \partial_\mu^2 A_1 + \beta A_1 |A_1|^2\ , \tag{38}$$

where we used the normalized condition $\tilde{\varphi}_{q_0}^{\mathrm{T}}\varphi_{q_0}=1$ and the coefficients are given by

$$\alpha = -\tilde{u}_{q_0}w_{q_0} \ , \tag{39}$$

$$d_1 = \frac{\eta_0}{2}(\tilde{u}_{q_0}u_{q_0}+\tilde{w}_{q_0}w_{q_0})+\xi_0\tilde{u}_{q_0}u_{q_0}+2\kappa_0\tilde{\theta}_{q_0}\theta_{q_0} \ , \tag{40}$$

$$d_2 = \xi_0(\tilde{u}_{q_0}w_{q_0}+\tilde{w}_{q_0}u_{q_0}) \ , \tag{41}$$

$$d_3 = \frac{\eta_0}{2}(\tilde{u}_{q_0}u_{q_0}+\tilde{w}_{q_0}w_{q_0})+\xi_0\tilde{w}_{q_0}w_{q_0}+2\kappa_0\tilde{\theta}_{q_0}\theta_{q_0} \ , \tag{42}$$

$$\begin{aligned}\beta = {} & 2\tilde{\theta}_{q_0}\nu_{q_0}(u_{q_0}+w_{q_0})\left(p_2\nu_{q_0}+\frac{p_1}{\theta_0}\theta_{q_0}\right) \\ & -(\tilde{u}_{q_0}+\tilde{w}_{q_0})\left(p_2'\nu_{q_0}^3+\frac{p_1'+p_2}{\theta_0}\nu_{q_0}^2\theta_{q_0}\right) \ .\end{aligned} \tag{43}$$

If we substitute Eqs.(28) and (29) to Eqs.(39)-(43), the leading terms of ϵ give

$$\alpha=\frac{1}{2} \ , \qquad d_1=d_3=\frac{\eta_0+\xi_0}{2} \ , \qquad d_2=-\xi_0 \ , \qquad \beta=\epsilon^{5/2}\bar{\beta} \ , \tag{44}$$

where

$$\bar{\beta}=\frac{\nu_0\theta_0^2}{128q_0^5J^8}\{4p_0^2p_1+2\nu_0\theta_0p_0(p_1'+2p_2)+\nu_0^2\theta_0^2p_2'\} \ . \tag{45}$$

It is notable that the coefficient β becomes higher order term of ϵ in our expansions in Eqs.(30) and (31). Then, we should introduce a rescaled amplitude as

$$\bar{A}_1=\epsilon^{5/4}A_1 \ . \tag{46}$$

If we use $\bar{A}_1$ instead of A_1, the TDGL equation is reduced to

$$\partial_\tau\bar{A}_1=\frac{1}{2}\bar{A}_1+d_1\partial_\xi^2\bar{A}_1+d_2\partial_\xi\partial_\mu\bar{A}_1+d_1\partial_\mu^2\bar{A}_1+\bar{\beta}\bar{A}_1|\bar{A}_1|^2 \ , \tag{47}$$

where all coefficients are independent of ϵ. If we use (ξ,ζ), Eq.(47) is rewritten as

$$\begin{aligned}\partial_\tau\bar{A}_1 = {} & \frac{1}{2}\bar{A}_1+\{(1+\tau^2)d_1-\tau d_2\}\partial_\xi^2\bar{A}_1 \\ & +(d_2-2\tau d_1)\partial_\xi\partial_\zeta\bar{A}_1+d_1\partial_\zeta^2\bar{A}_1+\bar{\beta}\bar{A}_1|\bar{A}_1|^2 \ .\end{aligned} \tag{48}$$

The scaling relation Eq.(46) is strange, because (i) $\bar{A}_1$ diverges as $\epsilon\to 0$ and (ii) higher order nonlinear terms seem to be relevant. However, we should keep in our mind that the point of $\epsilon\to 0$ is a singular point, where there is no steady state because of the absence of the balance between energy dissipation and input by shear. Therefore, our expansion cannot be used at $\epsilon=0$. In addition, as will be shown, higher order nonlinear terms are suppressed because the coefficients in front of the nonlinear terms depend on ϵ.

Let us compare the coefficients in Eq.(44) with the numerical calculations in which we numerically solve the eigenvalue problem Eq.(23) by LAPACK [68] and calculate α, d_1, d_2, d_3 and $\bar{\beta}=\beta/\epsilon^{5/2}$ from Eqs.(39)-(43). We have confirmed $\alpha\simeq 1/2$ in numerical calculation of Eq.(39). Figure 5 exhibits perfect agreement between the numerical results and our analytic calculation for the diffusion constants of (a) d_1 and (b) d_2, where the solid lines represent d_1 and d_2 in Eq.(44), and the open circles represent the numerical results of Eqs.(40) and (41), respectively. We have also confirmed that $d_3(=d_1)$ in Eq.(44) well explains the numerical results of Eq.(42). Figure 6 exhibits the

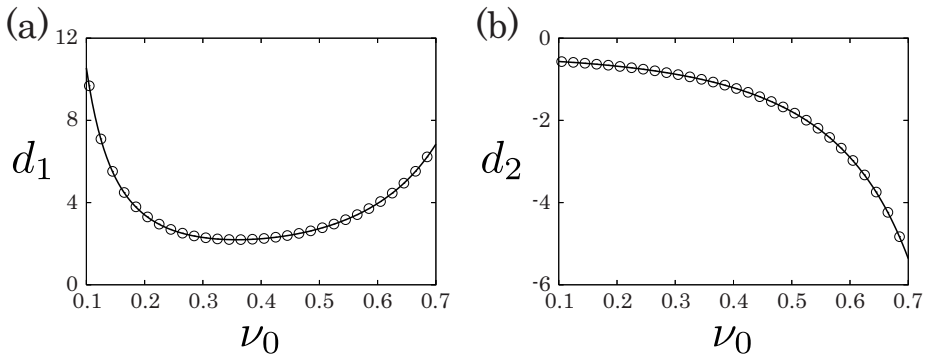

Fig. 5 (a) The solid line and the open circle represent d_1 given in Eq.(44) and the numerical result of Eq.(40). (b) The solid line and the open circle represent d_2 given in Eq.(44) and the numerical result of Eq.(41). Here, we have used $\epsilon = 0.01$.

result of $\bar{\beta}$, where the solid line and open circles represent Eq.(45) and the numerical result, respectively.

From these results, we find $\alpha = 1/2 > 0$ and $\bar{\beta} > 0$ in the range of $0.1 < \nu_0 < 0.7$. Therefore, the subcritical bifurcation is expected and we proceed our weakly nonlinear analysis to higher order expansions in the next section. It should be noted that the *bifurcation* from $\epsilon < 0$ cannot be realized in the hydrodynamic limit, because $\epsilon > 0$ by the definition of ϵ. Therefore, there is no hysteresis behavior even for the subcritical bifurcation.

4.3 Higher order expansions

The next nonzero terms are found at $O(\epsilon^4)$, where the coefficient of $e^{i\mathbf{q}_{\rm m}(\tau)\cdot\mathbf{z}}$ satisfies

$$\begin{aligned}\varphi_{q_0}\partial_\tau A_2 = {} & \mathcal{M}_2\varphi_{q_0}A_2 + \mathcal{D}_1\partial_\xi^2 A_2 + \mathcal{D}_2\partial_\xi\partial_\mu A_2 + \mathcal{D}_3\partial_\mu^2 A_2 \\ & + \mathcal{N}_3\left(A_1^2A_2^* + 2A_2|A_1|^2\right) \ , \end{aligned} \tag{49}$$

and at $O(\epsilon^5)$, the coefficient of $e^{i\mathbf{q}_{\rm m}(\tau)\cdot\mathbf{z}}$ satisfies

$$\begin{aligned}\varphi_{q_0}\partial_\tau A_3 = {} & \mathcal{M}_2\varphi_{q_0}A_3 + \mathcal{D}_1\partial_\xi^2 A_3 + \mathcal{D}_2\partial_\xi\partial_\mu A_3 + \mathcal{D}_3\partial_\mu^2 A_3 \\ & + \mathcal{N}_3\left(A_1^*A_2^2 + 2A_1|A_2|^2 + A_1^2A_3^* + 2|A_1|^2A_3\right) + \mathcal{N}_5 A_1|A_1|^4 \\ & + \mathcal{B}_1(A_1^2\partial_\xi^2 A_1^* + 2|A_1|^2\partial_\xi^2 A_1) + \mathcal{B}_2(A_1^2\partial_\xi\partial_\mu A_1^* + 2|A_1|^2\partial_\xi\partial_\mu A_1) \\ & + \mathcal{B}_3(A_1^2\partial_\mu^2 A_1^* + 2|A_1|^2\partial_\mu^2 A_1) + \mathcal{C}_1\{A_1^*(\partial_\xi A_1)^2 + 2A_1\partial_\xi A_1\partial_\xi A_1^*\} \\ & + \mathcal{C}_2\{A_1^*\partial_\xi A_1\partial_\mu A_1 + A_1\partial_\xi A_1^*\partial_\mu A_1 + A_1\partial_\xi A_1\partial_\mu A_1^*\} \\ & + \mathcal{C}_3\{A_1^*(\partial_\mu A_1)^2 + 2A_1\partial_\mu A_1\partial_\mu A_1^*\} \ , \end{aligned} \tag{50}$$

where the real vector $\mathcal{N}_5$ is given by

$$\mathcal{N}_5 = \begin{pmatrix} 0 \\ -2p_3'\nu_q^4\theta_q/\theta_0 \\ -2p_3'\nu_q^4\theta_q/\theta_0 \\ 4p_3\nu_q^3\theta_q(u_q+w_q)/\theta_0 \end{pmatrix} \ . \tag{51}$$

Although the real vectors $\mathcal{B}_1$, $\mathcal{B}_2$, $\mathcal{B}_3$, $\mathcal{C}_1$, $\mathcal{C}_2$ and $\mathcal{C}_3$ can be written explicitly, we do not need these analytic forms in the following discussion.

Now, we introduce a so-called *envelope function* as

$$\tilde{A}(\xi,\zeta,\tau) \equiv A_1(\xi,\zeta,\tau) + \epsilon A_2(\xi,\zeta,\tau) + \epsilon^2 A_3(\xi,\zeta,\tau) \ , \tag{52}$$

which is used by many authors to derive higher order amplitude equations [69,70,71]. If we sum up Eqs.(35), (49) and (50), we find

$$\begin{aligned}
\varphi_{q_0}\partial_\tau \tilde{A} = {} & \mathcal{M}_2\varphi_{q_0}\tilde{A} + \mathcal{D}_1\partial_\xi^2\tilde{A} + \mathcal{D}_2\partial_\xi\partial_\mu\tilde{A} + \mathcal{D}_3\partial_\mu^2\tilde{A} + \mathcal{N}_3\tilde{A}|\tilde{A}|^2 + \epsilon^2\mathcal{N}_5\tilde{A}|\tilde{A}|^4 \\
& + \epsilon^2\Big[\mathcal{B}_1(\tilde{A}^2\partial_\xi^2\tilde{A}^* + 2|\tilde{A}|^2\partial_\xi^2\tilde{A}) + \mathcal{B}_2(\tilde{A}^2\partial_\xi\partial_\mu\tilde{A}^* + 2|\tilde{A}|^2\partial_\xi\partial_\mu\tilde{A}) \\
& + \mathcal{B}_3(\tilde{A}^2\partial_\mu^2\tilde{A}^* + 2|\tilde{A}|^2\partial_\mu^2\tilde{A}) + \mathcal{C}_1\{\tilde{A}^*(\partial_\xi\tilde{A})^2 + 2\tilde{A}\partial_\xi\tilde{A}\partial_\xi\tilde{A}^*\} \\
& + \mathcal{C}_2\{\tilde{A}^*\partial_\xi\tilde{A}\partial_\mu\tilde{A} + \tilde{A}\partial_\xi\tilde{A}^*\partial_\mu\tilde{A} + \tilde{A}\partial_\xi\tilde{A}\partial_\mu\tilde{A}^*\} \\
& + \mathcal{C}_3\{\tilde{A}^*(\partial_\mu\tilde{A})^2 + 2\tilde{A}\partial_\mu\tilde{A}\partial_\mu\tilde{A}^*\}\Big]
\end{aligned} \tag{53}$$

at $O(\epsilon^3)$. If we multiply $\tilde{\varphi}_{q_0}^{\mathrm{T}}$ to Eq.(53), we find

$$\begin{aligned}
\partial_\tau \tilde{A} = {} & \alpha\tilde{A} + d_1\partial_\xi^2\tilde{A} + d_2\partial_\xi\partial_\mu\tilde{A} + d_3\partial_\mu^2\tilde{A} + \beta\tilde{A}|\tilde{A}|^2 + \epsilon^2\gamma\tilde{A}|\tilde{A}|^4 \\
& + \epsilon^2\Big[b_1(\tilde{A}^2\partial_\xi^2\tilde{A}^* + 2|\tilde{A}|^2\partial_\xi^2\tilde{A}) + b_2(\tilde{A}^2\partial_\xi\partial_\mu\tilde{A}^* + 2|\tilde{A}|^2\partial_\xi\partial_\mu\tilde{A}) \\
& + b_3(\tilde{A}^2\partial_\mu^2\tilde{A}^* + 2|\tilde{A}|^2\partial_\mu^2\tilde{A}) + c_1\{\tilde{A}^*(\partial_\xi\tilde{A})^2 + 2\tilde{A}\partial_\xi\tilde{A}\partial_\xi\tilde{A}^*\} \\
& + c_2\{\tilde{A}^*\partial_\xi\tilde{A}\partial_\mu\tilde{A} + \tilde{A}\partial_\xi\tilde{A}^*\partial_\mu\tilde{A} + \tilde{A}\partial_\xi\tilde{A}\partial_\mu\tilde{A}^*\} \\
& + c_3\{\tilde{A}^*(\partial_\mu\tilde{A})^2 + 2\tilde{A}\partial_\mu\tilde{A}\partial_\mu\tilde{A}^*\}\Big],
\end{aligned} \tag{54}$$

where $b_j \equiv \tilde{\varphi}_{q_0}^{\mathrm{T}}\mathcal{B}_j$, $c_j \equiv \tilde{\varphi}_{q_0}^{\mathrm{T}}\mathcal{C}_j$ $(j=1,2,3)$ and

$$\gamma = \frac{2}{\theta_0}\nu_q^3\theta_q\left\{2p_3\tilde{\theta}_q(u_q+w_q) - p_3'(\tilde{u}_q+\tilde{w}_q)\nu_q\right\} \ . \tag{55}$$

If we substitute Eqs.(28) and (29) to Eq.(55), the leading terms of ϵ give

$$\gamma = \epsilon^{7/2}\bar{\gamma} \ , \qquad b_j = \epsilon^2\bar{b}_j \ , \qquad c_j = \epsilon^2\bar{c}_j \ , \tag{56}$$

where

$$\bar{\gamma} = \frac{\nu_0^3\theta_0^4 p_0}{256 q_0^7 J^{12}}\{2p_0p_3 + \nu_0\theta_0 p_3'\} \ . \tag{57}$$

Although $\bar{b}_j$ and $\bar{c}_j$ $(j=1,2,3)$ can be written explicitly, we do not need such analytic forms in later discussion. Then, we introduce $\check{A} = \epsilon^{5/4}\tilde{A}$ and find the TDGL equation of $\check{A}$ as

$$\begin{aligned}
\partial_\tau \check{A} = {} & \frac{1}{2}\check{A} + d_1\partial_\xi^2\check{A} + d_2\partial_\xi\partial_\mu\check{A} + d_1\partial_\mu^2\check{A} + \bar{\beta}\check{A}|\check{A}|^2 + \epsilon^{1/2}\bar{\gamma}\check{A}|\check{A}|^4 \\
& + \epsilon^{3/2}\Big[\bar{b}_1(\check{A}^2\partial_\xi^2\check{A}^* + 2|\check{A}|^2\partial_\xi^2\check{A}) + \bar{b}_2(\check{A}^2\partial_\xi\partial_\mu\check{A}^* + 2|\check{A}|^2\partial_\xi\partial_\mu\check{A}) \\
& + \bar{b}_3(\check{A}^2\partial_\mu^2\check{A}^* + 2|\check{A}|^2\partial_\mu^2\check{A}) + \bar{c}_1\{\check{A}^*(\partial_\xi\check{A})^2 + 2\check{A}\partial_\xi\check{A}\partial_\xi\check{A}^*\} \\
& + \bar{c}_2\{\check{A}^*\partial_\xi\check{A}\partial_\mu\check{A} + \check{A}\partial_\xi\check{A}^*\partial_\mu\check{A} + \check{A}\partial_\xi\check{A}\partial_\mu\check{A}^*\} \\
& + \bar{c}_3\{\check{A}^*(\partial_\mu\check{A})^2 + 2\check{A}\partial_\mu\check{A}\partial_\mu\check{A}^*\}\Big] \ .
\end{aligned} \tag{58}$$

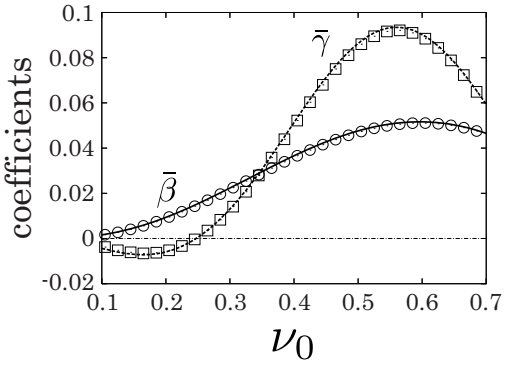

Fig. 6 The solid and the broken lines represent Eqs.(45) and (57), respectively. The open circles and the open squares represent the numerical results of $\bar{\beta}$ and $\bar{\gamma}$, respectively. Here, we have used $\epsilon = 0.01$.

Because $\bar{b}_j$ and $\bar{c}_j$ $(j = 1, 2, 3)$ do not include ϵ, the terms in the second to fifth lines in Eq.(58) are negligible compared to the terms in the first line. Thus, we obtain the closed TDGL equation including the term of $\check{A}|\check{A}|^4$ as the equation in the first line of Eq.(58).

Let us compare the analytic form Eq.(57) with the numerical calculation in which we numerically solve the eigenvalue problem Eq.(23) by LAPACK [68] and calculate $\bar{\gamma} = \gamma/\epsilon^{7/2}$ from Eq.(55). Figure 6 exhibits the complete agreement of $\bar{\gamma}$ obtained by the two different methods, where the broken line and the open square represent Eq.(57) and the numerical result, respectively.

From this result, if $0.1 < \nu_0 < 0.25$, the growth of disturbance is inhibited by the nonlinear term $\epsilon^{1/2}\bar{\gamma}\check{A}|\check{A}|^4$ and finite steady amplitude can be observed. For $\nu_0 > 0.25$, we need to calculate higher order expansions, however, such a calculation is too complicated to perform in this paper.

5 Discussion and Conclusion

Now, let us discuss our results. There are three points to be argued in this paper.

First, to derive the TDGL equation Eq.(47), we have introduced the amplitude $\bar{A}_1 = \epsilon^{5/4}A_1$. In this case, the amplitude of the disturbance field $\hat{\phi}$ satisfies

$$\hat{\phi} \ \propto \ \epsilon^{-1/4}\bar{A}_1(\xi,\zeta,\tau) + \epsilon^{3/4}\bar{A}_2(\xi,\zeta,\tau) + \epsilon^{7/4}\bar{A}_3(\xi,\zeta,\tau) + \dots \ , \tag{59}$$

where $\bar{A}_2$ and $\bar{A}_3$ are $\epsilon^{5/4}A_2$ and $\epsilon^{5/4}A_3$, respectively. Thus, as stated in Sec.4.2, the leading term $\epsilon^{-1/4}\bar{A}_1$ diverges in the limit of $\epsilon \to 0$. Although this singular behavior might be possible because $\epsilon = 0$ is an unreachable singular point, the numerical simulation of Eqs.(1)-(3) is necessary to confirm what kind of singularities appear in the limit $\epsilon \to 0$.

Second, $\epsilon^{-1/4}\bar{A}_1$ in Eq.(59) indicates the nonlinear term

$$\epsilon^{-(2m+1)/4}\bar{A}_1|\bar{A}_1|^{2m} \qquad (m = 1, 2, \dots) \tag{60}$$

which increases with the magnitude $O(\epsilon^{-(2m+1)/4})$ as m increases. However, such nonlinear terms appear in higher expansions of ϵ, and the coefficients of Eq.(60) may include

ϵ as we have seen in Eqs.(44) and (56). Thus, we may use this singular expansions near $\epsilon = 0$.

Third, let us compare our results with the previous studies [49,50]. Our result implies that the diffusive coupling terms should be relevant and the coefficient of $\check{A}|\check{A}|^4$ can be calculated explicitly based on a systematic perturbation method in terms of small ϵ. If we analyze a finite size system around most unstable mode, the result becomes similar to that of the previous studies. However, the scaling of time scale, where L/U or the inverse of the growth rate is a relevant time scale, becomes subtle in such a case. This should be clarified in future, though we have avoided such a subtle point in this paper.

In conclusion, we have derived the TDGL equation starting from a set of granular hydrodynamic equations. From our result, we find $\alpha = 1/2 > 0$ and $\bar{\beta} > 0$ in the range of $0.1 < \nu_0 < 0.7$. If $0.1 < \nu_0 < 0.25$, the growth of disturbance is inhibited by the nonlinear term $\epsilon^{1/2}\bar{\gamma}\check{A}|\check{A}|^4$ and finite steady amplitude is predicted. However, in the case of $\nu_0 > 0.25$, higher order expansions are necessary and such a calculation should be performed in a future work.

Acknowledgements We would like to thank M. Otsuki, H. Nakao and M. Alam for fruitful discussions, and S. Luding for his encouragement of the initiation of this study. This work was supported by the Global COE Program "The Next Generation of Physics, Spun from Universality & Emergence" from the Ministry of Education, Culture, Sports, Science and Technology (MEXT) of Japan, the Research Fellowship of the Japan Society for the Promotion of Science for Young Scientists (JSPS), and the Grant-in-Aid of MEXT (Grants No.21015016, 21540384 and 21.1958).

Appendix A Derivation of the coefficients in Table 1

In this Appendix, we derive the coefficients in Table 1 by using the dimensionless quantities based on the kinetic theory [43].

At first, the energy sources $\chi_{\alpha\alpha}$ and χ_3 for smooth disks ($\beta = -1$ in Ref.[43]) are respectively given by

$$\chi_{\alpha\alpha} = -\frac{\xi(1-e)}{2d^2}\left[8T - 3\pi^{1/2}dT^{1/2}(\nabla\cdot\mathbf{u})\right] \tag{61}$$

and $\chi_{33} = 0$, where d, $T \equiv m\langle(\mathbf{c}-\mathbf{u})^2\rangle/2$ and $\mathbf{u} = U\mathbf{v}/2$ are the diameter of a disk, the granular temperature and the velocity field, respectively. It should be noted that we adopt the different definition for the granular temperature T from Ref.[43] to keep the dimension of the energy. In Eq.(61), the bulk viscosity ξ is given by

$$\xi = \frac{4m}{\pi^{3/2}d}(1+e)\nu^2 g(\nu)T^{1/2} \ . \tag{62}$$

where ν and $g(\nu)$ is the area fraction and the radial distribution function at contact, respectively. Thus, the factor of Eq.(61) is given by

$$-\frac{\xi(1-e)}{2\sigma^2} = -\frac{2m\nu^2(1-e^2)}{\pi^{3/2}d^3}g(\nu)T^{1/2} \ . \tag{63}$$

If we introduce the mass density of the system $\rho = 4m\nu/(\pi d^2)$ and the mass density of a disk $\rho_p = 4m/(\pi d^2)$, Eq.(61) is reduced to

$$\chi_{\alpha\alpha} = -\frac{1-e^2}{2\rho_p\pi^{1/2}d}\rho^2 g(\nu)T^{1/2}\left[8T - 3\pi^{1/2}dT^{1/2}(\nabla\cdot\mathbf{u})\right] \ , \tag{64}$$

and the energy loss rate is given by

$$\chi = -\frac{\chi_{\alpha\alpha}}{2} = \frac{1-e^2}{4\rho_p \pi^{1/2} d} \rho^2 g(\nu) T^{1/2} \left[8T - 3\pi^{1/2} d T^{1/2} (\nabla \cdot \mathbf{u}) \right] \ . \tag{65}$$

Next, we consider the pressure tensor $P_{ij} = \rho T \delta_{ij} + \rho a_{ij} + \Theta_{ij}$, where ρa_{ij} and Θ_{ij} are respectively given by

$$\rho a_{ij} = -\frac{2mT^{1/2}}{\pi^{1/2} d g(\nu)(5-3r)} \left[1 + \nu g(\nu)(3r-2) r \right] D'_{ij} \ , \tag{66}$$

$$\Theta_{ij} = (2\rho T \nu g(\nu) r - \xi \nabla \cdot \mathbf{u}) \delta_{ij} - \xi D'_{ij} + \nu g(\nu) r \rho a_{ij} \ , \tag{67}$$

where we have introduced $r = (1+e)/2$. Then, we find

$$P_{ij} = \left[p - \xi \nabla \cdot \mathbf{u} \right] \delta_{ij} - \xi D'_{ij} + \left[1 + r\nu g(\nu) \right] \rho a_{ij} \ , \tag{68}$$

where we have introduced the static pressure $p = \rho T \left[1 + (1+e)\nu g(\nu) \right]$. The second and third terms on the right-hand-side of Eq.(68) can be rewritten as $\xi D'_{ij} - \left[1 + r\nu g(\nu) \right] \rho a_{ij} \equiv \eta D'_{ij}$, where the shear viscosity η is given by

$$\eta = \frac{4mT^{1/2}}{\pi^{1/2} d} \left[\frac{g(\nu)^{-1}}{7-3e} + \frac{(1+e)(3e+1)}{4(7-3e)} \nu + \left[\frac{(1+e)(3e-1)}{8(7-3e)} + \frac{1}{\pi} \right] (1+e) \nu^2 g(\nu) \right] \ . \tag{69}$$

Therefore, we find $P_{ij} = \left[p - \xi \nabla \cdot \mathbf{u} \right] \delta_{ij} - \eta D'_{ij}$. It should be noted that Eq.(70) in Ref.[43] should be multiplied by rm.

Next, we consider the translational energy flux $q_\alpha = \rho a_{\alpha\beta\beta}/2 + \Theta_{\alpha\beta\beta}/2$, where $\rho a_{\alpha\beta\beta}/2$ and $\Theta_{\alpha\beta\beta}/2$ are given by Eq.(89) and (100) in Ref.[43], respectively. From Eq.(100) in Ref.[43], we rewrite q_α as

$$\begin{aligned} q_\alpha &= \frac{1}{2} \rho a_{\alpha\beta\beta} - \xi \nabla T + \frac{3}{2} r \nu g(\nu) \cdot \frac{1}{2} \rho a_{\alpha\beta\beta} \\ &= \left(1 + \frac{3}{2} r \nu g(\nu) \right) \frac{1}{2} \rho a_{\alpha\beta\beta} - \xi \nabla T \ . \end{aligned} \tag{70}$$

We introduce κ_ρ and λ_ρ as $\frac{1}{2} \rho a_{\alpha\beta\beta} \equiv -\kappa_\rho \nabla T - \lambda_\rho \nabla \rho$, where κ_ρ and λ_ρ are given by

$$\kappa_\rho = \frac{4mT^{1/2}}{\sigma g(\nu) r (17-15r) \pi^{1/2}} \left[1 + \frac{3}{2} \nu g(\nu) r^2 (4r-3) \right] \ , \tag{71}$$

$$\lambda_\rho = -\frac{3\sigma \pi^{1/2} (2r-1)(1-r)}{2\nu g(\nu)(17-15r)} T^{3/2} \frac{d(\nu^2 g(\nu))}{d\nu} \ , \tag{72}$$

respectively. If we write the energy flux q_α as $q_\alpha \equiv -\kappa \nabla T - \lambda \nabla \rho$, we obtain the heat conductivity κ

$$\begin{aligned} \kappa &= \kappa_\rho \left(1 + \frac{3}{2} r \nu g(\nu) \right) + \xi \\ &= \frac{16mT^{1/2}}{\sigma \pi^{1/2}} \Big[\frac{g(\nu)^{-1}}{(1+e)(19-15e)} + \frac{3(2e^2+e+1)}{8(19-15e)} \nu \\ &\quad + \left\{ \frac{9(1+e)^2(2e-1)}{32(19-15e)} + \frac{1}{4\pi} \right\} (1+e) \nu^2 g(\nu) \Big] \ , \end{aligned} \tag{73}$$

and the coefficient associated with the gradient of density λ

$$\lambda = \lambda_\rho \left(1 + \frac{3}{2} r \nu g(\nu) \right) = -\frac{3\sigma \pi^{1/2} e(1-e)}{8(19-15e)} \left[4g(\nu)^{-1} + 3(1+e)\nu \right] \frac{1}{\nu} \frac{d(\nu^2 g(\nu))}{d\nu} T^{3/2} \ . \tag{74}$$

We should note that the third term on the right hand side of Eq.(73) differs from our paper [12]. Indeed, the coefficient $1/4\pi$ in the last term on the right hand side of Eq. (73) is different from $1/2\pi$.

Now, we non-dimensionalize the static pressure, transport coefficients and the coefficient associated with the gradient of density with the aid of m, d and $U/2$ as

$$p = \rho_p \left(\frac{U}{2}\right)^2 p^*(\nu)\theta \ , \tag{75}$$

$$\xi = \rho_p d \frac{U}{2} \xi^*(\nu)\theta^{1/2} \ , \tag{76}$$

$$\eta = \rho_p d \frac{U}{2} \eta^*(\nu)\theta^{1/2} \ , \tag{77}$$

$$\kappa = \rho_p d U \kappa^*(\nu)\theta^{1/2} \ , \tag{78}$$

$$\lambda = d \left(\frac{U}{2}\right)^3 \lambda^*(\nu)\theta^{3/2} \ , \tag{79}$$

where $p^*(\nu)$, $\xi^*(\nu)$, $\eta^*(\nu)$, $\kappa^*(\nu)$ and $\lambda^*(\nu)$ are dimensionless quantities listed in Table 1.

Appendix B The Taylor expansion of the functions in Table 1

The functions in Table 1 are expanded into the Taylor series as

$$g(\nu) = g_0 + g_1\nu + g_2\nu^2 + \dots \ , \tag{80}$$

$$\theta_0\nu^{-1}p^*(\nu) = p_0 + p_1\nu + p_2\nu^2 + \dots \ , \tag{81}$$

$$\theta_0^{1/2}\nu^{-1}\xi^*(\nu) = \xi_0 + \xi_1\nu + \xi_2\nu^2 + \dots \ , \tag{82}$$

$$\theta_0^{1/2}\nu^{-1}\eta^*(\nu) = \eta_0 + \eta_1\nu + \eta_2\nu^2 + \dots \ , \tag{83}$$

$$\theta_0^{1/2}\nu^{-1}\kappa^*(\nu) = \kappa_0 + \kappa_1\nu + \kappa_2\nu^2 + \dots \ , \tag{84}$$

$$\theta_0^{3/2}\nu^{-1}\lambda^*(\nu) = \lambda_0 + \lambda_1\nu + \lambda_2\nu^2 + \dots \ . \tag{85}$$

Similarly, the derivatives are also expanded into the Taylor series as

$$\theta_0\nu^{-1}\frac{dp^*(\nu)}{d\nu} = p_0' + p_1'\nu + p_2'\nu^2 + \dots \ , \tag{86}$$

$$\theta_0^{1/2}\nu^{-1}\frac{d\xi^*(\nu)}{d\nu} = \xi_0' + \xi_1'\nu + \xi_2'\nu^2 + \dots \ , \tag{87}$$

$$\theta_0^{1/2}\nu^{-1}\frac{d\eta^*(\nu)}{d\nu} = \eta_0' + \eta_1'\nu + \eta_2'\nu^2 + \dots \ , \tag{88}$$

$$\theta_0^{1/2}\nu^{-1}\frac{d\kappa^*(\nu)}{d\nu} = \kappa_0' + \kappa_1'\nu + \kappa_2'\nu^2 + \dots \ . \tag{89}$$

In the following, we show the explicit expressions of the coefficients which are used in the text. The coefficients associated with the radial distribution function are given by

$$g_1 = \frac{25 - 7\nu_0}{16(1-\nu_0)^3} \ , \qquad g_2 = \frac{34 - 7\nu_0}{16(1-\nu_0)^4} \ , \qquad g_3 = \frac{43 - 7\nu_0}{16(1-\nu_0)^5} \ . \tag{90}$$

The coefficients associated with the static pressure are given by

$$p_1 = \frac{1}{2}(1+e)(g_0 + \nu_0 g_1)\theta_0 \ , \tag{91}$$

$$p_2 = \frac{1}{2}(1+e)(g_1 + \nu_0 g_2)\theta_0 \ , \tag{92}$$

$$p_3 = \frac{1}{2}(1+e)(g_2 + \nu_0 g_3)\theta_0 \ . \tag{93}$$

The coefficients associated with viscosity are given by

$$\xi_1 = \frac{1+e}{\sqrt{2\pi}}(g_0 + \nu_0 g_1)\theta_0^{1/2} \ , \tag{94}$$

$$\eta_1 = \left\{ a_\eta - \frac{b_\eta}{(\nu_0 g_0)^2} \right\} (g_0 + \nu_0 g_1)\theta_0^{1/2} \ , \tag{95}$$

where we have introduced

$$a_\eta = \sqrt{\frac{\pi}{2}} \left(\frac{(1+e)(3e-1)}{8(7-3e)} + \frac{1}{\pi} \right) (1+e) \ , \tag{96}$$

$$b_\eta = \sqrt{\frac{\pi}{2}} \frac{1}{7-3e} \ . \tag{97}$$

The coefficients associated with the heat conductivity are given by

$$\kappa_1 = \left\{ a_\kappa - \frac{b_\kappa}{(\nu_0 g_0)^2} \right\} (g_0 + \nu_0 g_1)\theta_0^{1/2} \ , \tag{98}$$

where we have introduced

$$a_\kappa = \sqrt{2\pi} \left(\frac{9(1+e)(2e-1)}{32(19-15e)} + \frac{1}{4\pi} \right) (1+e) \ , \tag{99}$$

$$b_\kappa = \frac{\sqrt{2\pi}}{(1+e)(19-15e)} \ . \tag{100}$$

The coefficients associated with the derivative of the static pressure are given by

$$p_0' = \frac{1}{2\nu_0} \left\{ (1+e)\nu_0 \left(2g_0 + \nu_0 g_1 \right) + 1 \right\} \theta_0 \ , \tag{101}$$

$$p_1' = \frac{1}{2\nu_0^2} \left\{ (1+e)\nu_0^2 \left(3g_1 + 2\nu_0 g_2 \right) - 1 \right\} \theta_0 \ , \tag{102}$$

$$p_2' = \frac{1}{2\nu_0^3} \left\{ (1+e)\nu_0^3 \left(4g_2 + 3\nu_0 g_3 \right) + 1 \right\} \theta_0 \ , \tag{103}$$

$$p_3' = \frac{1}{2\nu_0^4} \left\{ (1+e)\nu_0^4 \left(5g_3 + 4\nu_0 g_4 \right) - 1 \right\} \theta_0 \ . \tag{104}$$

The coefficients associated with the derivative of viscosity are given by

$$\xi_0' = \frac{1+e}{\sqrt{2\pi}}(2g_0 + \nu_0 g_1)\theta_0^{1/2} \ , \tag{105}$$

$$\eta_0' = \frac{1}{\nu_0 g_0^2} \left[-a_\eta g_1 + g_0^2 \left\{ c_\eta \nu_0 \left(2g_0 + \nu_0 g_1 \right) + b_\eta \right\} \right] \theta_0^{1/2} \ . \tag{106}$$

The coefficients associated with the derivative of the heat conductivity are given by

$$\kappa_0' = \frac{1}{\nu_0 g_0^2} \left[-a_\kappa g_1 + g_0^2 \left\{ c_\kappa \nu_0 \left(2g_0 + \nu_0 g_1 \right) + b_\kappa \right\} \right] \theta_0^{1/2} \ , \tag{107}$$

$$\kappa_1' = \frac{1}{\nu_0^2 g_0^3} \left[a_\kappa \left\{ 2\nu_0 g_1^2 + g_0 \left(g_1 - 2\nu_0 g_2 \right) \right\} + g_0^3 \left\{ c_\kappa \nu_0^2 \left(3g_1 + 2\nu_0 g_2 \right) - b_\kappa \right\} \right] \theta_0^{1/2} \ . \tag{108}$$

Appendix C Perturbative calculation of the eigenvalue problem

In this appendix, we perturbatively solve the eigenvalue problem

$$\mathcal{L}_q \varphi_q^{(j)} = \sigma^{(j)} \varphi_q^{(j)} \ , \tag{109}$$

where $j = 1, 2, 3, 4$. At first, we expand $\mathcal{L}_q$, $\varphi_q^{(j)}$ and $\sigma^{(j)}$ into the series of ϵ as

$$\mathcal{L}_q = \mathcal{L}_0 + \epsilon\mathcal{L}_1 + \epsilon^2\mathcal{L}_2 + \epsilon^3\mathcal{L}_3 + \dots \ , \tag{110}$$

$$\varphi_q^{(j)} = \varphi_0^{(j)} + \epsilon\varphi_1^{(j)} + \epsilon^2\varphi_2^{(j)} + \epsilon^3\varphi_3^{(j)} + \dots \ , \tag{111}$$

$$\sigma^{(j)} = \sigma_0^{(j)} + \epsilon i\sigma_1^{(j)} + \epsilon^2\sigma_2^{(j)} + \epsilon^3 i\sigma_3^{(j)} + \dots \ , \tag{112}$$

where i is the imaginary unit and

$$\mathcal{L}_0 = \mathbf{0} \ , \tag{113}$$

$$\mathcal{L}_1 = q\begin{pmatrix} 0 & \nu_0 & \nu_0 & 0 \\ -p_0' & 0 & 0 & -p_0/\theta_0 \\ -p_0' & 0 & 0 & -p_0/\theta_0 \\ 0 & 2p_0 & 2p_0 & 0 \end{pmatrix} \ , \tag{114}$$

$$\mathcal{L}_2 = \begin{pmatrix} 0 & 0 & 0 & 0 \\ 0 & -q^2(\xi_0+\eta_0) & -q^2\xi_0 - 1 & 0 \\ 0 & -q^2\xi_0 & -q^2(\xi_0+\eta_0) & 0 \\ 0 & 0 & 0 & -4q^2\kappa_0 \end{pmatrix} \ . \tag{115}$$

Because of $\mathcal{L}_0 = \mathbf{0}$, arbitrary $\varphi_0^{(j)}$ are degenerated to the zero eigenvalue $\sigma_0^{(j)} = 0$. Thus, we need higher order expansions of Eq.(109) to determine the undegenerated forms of $\varphi_0^{(j)}$.

At $O(\epsilon)$ of Eq.(109), we find

$$\mathcal{L}_1\varphi_0^{(j)} = i\sigma_1^{(j)}\varphi_0^{(j)} \ . \tag{116}$$

From Eq.(116), we find the eigenvalues

$$i\sigma_1^{(1)} = i\sigma_1^{(2)} = 0 \ , \qquad i\sigma_1^{(3)} = -i\sigma_1^{(4)} = i\sqrt{\frac{2}{\theta_0}}qJ \ , \tag{117}$$

where we have defined the constant J as

$$J \equiv \sqrt{2p_0^2 + \nu_0\theta_0 p_0'} \ . \tag{118}$$

The eigenvalues Eq.(117) are given by the eigenvectors

$$\varphi_0^{(1)} = \left(0, \frac{1}{\sqrt{2}}, -\frac{1}{\sqrt{2}}, 0\right)^{\mathrm{T}} \ , \tag{119}$$

$$\varphi_0^{(2)} = \left(-\frac{p_0}{J}, 0, 0, \frac{\theta_0 p_0'}{J}\right)^{\mathrm{T}} \ , \tag{120}$$

$$\varphi_0^{(3)} = \left(\frac{\nu_0}{\sqrt{2}J}, \frac{i}{2\theta_0^{1/2}}, \frac{i}{2\theta_0^{1/2}}, \frac{\sqrt{2}p_0}{J}\right)^{\mathrm{T}} \ , \tag{121}$$

$$\varphi_0^{(4)} = \left(\frac{\nu_0}{\sqrt{2}J}, -\frac{i}{2\theta_0^{1/2}}, -\frac{i}{2\theta_0^{1/2}}, \frac{\sqrt{2}p_0}{J}\right)^{\mathrm{T}} \ , \tag{122}$$

respectively. We also find the corresponding left eigenvectors

$$\tilde{\varphi}_0^{(1)} = \left(0, \frac{1}{\sqrt{2}}, -\frac{1}{\sqrt{2}}, 0\right) \ , \tag{123}$$

$$\tilde{\varphi}_0^{(2)} = \left(-\frac{2p_0}{J}, 0, 0, \frac{\nu_0}{J}\right) \ , \tag{124}$$

$$\tilde{\varphi}_0^{(3)} = \left(\frac{\theta_0 p_0'}{\sqrt{2}J}, -\frac{i\theta_0^{1/2}}{2}, -\frac{i\theta_0^{1/2}}{2}, \frac{p_0}{\sqrt{2}J}\right) \ , \tag{125}$$

$$\tilde{\varphi}_0^{(4)} = \left(\frac{\theta_0 p_0'}{\sqrt{2}J}, \frac{i\theta_0^{1/2}}{2}, \frac{i\theta_0^{1/2}}{2}, \frac{p_0}{\sqrt{2}J}\right) \ . \tag{126}$$

The eigenvectors Eqs.(119)-(126) are orthogonal and normalized as

$$\tilde{\varphi}_0^{(j)}\varphi_0^{(k)} = \delta_{jk} \ , \tag{127}$$

where $j,k = 1,2,3,4$ and δ_{jk} is the Kronecker delta. Because the critical eigenvalue is a real number, i.e. zero, we are interested in the case $\sigma_1^{(1)} = \sigma_1^{(2)} = 0$. However, $\varphi_0^{(1)}$ and $\varphi_0^{(2)}$ are degenerated, thus we rewrite Eq.(111) as

$$\varphi_q^{(l)} = \left\{ a_1^{(l)}\varphi_0^{(1)} + a_2^{(l)}\varphi_0^{(2)} \right\} + \epsilon\varphi_1^{(l)} + \epsilon^2\varphi_2^{(l)} + \epsilon^3\varphi_3^{(l)} + \dots \ , \tag{128}$$

where $l = 1,2$ and the coefficients $a_1^{(l)}$ and $a_2^{(l)}$ are determined later.

At $O(\epsilon^2)$ of Eq.(109), we find

$$\mathcal{L}_1\varphi_1^{(l)} + \mathcal{L}_2\left\{ a_1^{(l)}\varphi_0^{(1)} + a_2^{(l)}\varphi_0^{(2)} \right\} = \sigma_2^{(l)}\left\{ a_1^{(l)}\varphi_0^{(1)} + a_2^{(l)}\varphi_0^{(2)} \right\} \ . \tag{129}$$

If we multiply $\tilde{\varphi}_0^{(l)}$ $(l = 1,2)$ to Eq.(129), respectively, we find

$$\begin{pmatrix} \tilde{\varphi}_0^{(1)}\mathcal{L}_2\varphi_0^{(1)} & \tilde{\varphi}_0^{(1)}\mathcal{L}_2\varphi_0^{(2)} \\ \tilde{\varphi}_0^{(2)}\mathcal{L}_2\varphi_0^{(1)} & \tilde{\varphi}_0^{(2)}\mathcal{L}_2\varphi_0^{(2)} \end{pmatrix} \begin{pmatrix} a_1^{(l)} \\ a_2^{(l)} \end{pmatrix} = \sigma_2^{(l)} \begin{pmatrix} a_1^{(l)} \\ a_2^{(l)} \end{pmatrix} \ . \tag{130}$$

From Eq.(130), we find that

$$\sigma_2^{(1)} = \frac{1}{2} - q^2\eta_0 \ , \qquad \sigma_2^{(2)} = -\frac{4q^2\nu_0\theta_0 p_0'\kappa_0}{J^2} \tag{131}$$

are given by $(a_1^{(1)}, a_2^{(1)}) = (1,0)$ and $(a_1^{(2)}, a_2^{(2)}) = (0,1)$, respectively.

Because p_0' is always positive, $\sigma_2^{(2)} < 0$. Therefore, the growth rate of disturbance is determined by $\sigma_2^{(1)}$ and the unstable mode $\mathbf{k}(t) = q\epsilon(1, 1+\tau)$ is found in the range

$$0 < q < \frac{1}{\sqrt{2\eta_0}} \ . \tag{132}$$

Indeed, if q satisfies Eq.(132), $\sigma_2^{(1)} > 0$.

Let us compare the results of our perturbative calculation Eqs.(117) and (131) with results of numerical calculation of $\sigma^{(j)}$. Figure 7 displays (a) real and (b) imaginary parts of $\sigma^{(j)}$. In this figure, the solid and broken lines represent the analytic forms of $\sigma^{(j)}$ and points are numerical results of the eigenvalue problem Eq.(109) obtained by LAPACK [68]. From these results, the behaviors of $\sigma^{(1)}$ and $\sigma^{(2)}$ are well explained in the range $0 < \epsilon < 0.1$.

If we choose $(a_1^{(1)}, a_2^{(1)}) = (1,0)$, Eq.(129) is reduced to

$$\mathcal{L}_1\varphi_1^{(1)} = \left\{ \sigma_2^{(1)} - \mathcal{L}_2 \right\}\varphi_0^{(1)} \ . \tag{133}$$

Then, if we multiply $\varphi_0^{(n)}\tilde{\varphi}_0^{(n)}$ $(n = 3,4)$ to Eq.(133), we can find $\varphi_1^{(1)}$ in the form

$$\varphi_1^{(1)} = \psi_1 + C\varphi_0^{(2)} \ , \tag{134}$$

where C is a constant and ψ_1 is defined as

$$\psi_1 \equiv -\sum_{n=3,4} \frac{1}{i\sigma_1^{(n)}}\varphi_0^{(n)}(\tilde{\varphi}_0^{(n)}\mathcal{L}_2\varphi_0^{(1)}) = \left(\frac{\nu_0\theta_0}{2\sqrt{2}qJ^2}, 0, 0, \frac{\theta_0 p_0}{\sqrt{2}qJ^2} \right)^{\mathrm{T}} \ . \tag{135}$$

At $O(\epsilon^3)$ of Eq.(109), we find

$$\mathcal{L}_1\varphi_2^{(1)} + \mathcal{L}_2\varphi_1^{(1)} + \mathcal{L}_3\varphi_0^{(1)} = i\sigma_3^{(1)}\varphi_0^{(1)} + \sigma_2^{(1)}\varphi_1^{(1)} \ . \tag{136}$$

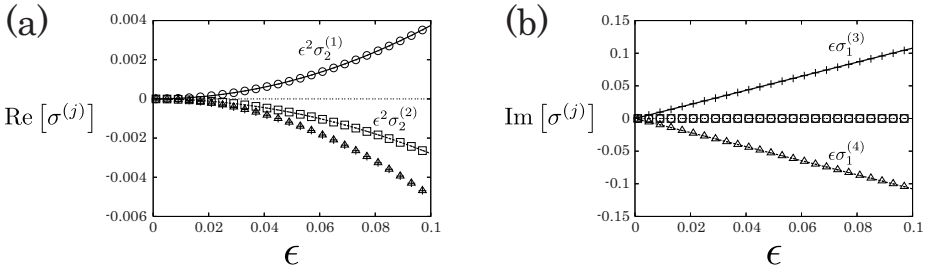

Fig. 7 The results of perturbative calculation Eqs.(117) and (131), and numerical results of $\sigma^{(j)}$: (a) The solid and broken lines are $\epsilon^2\sigma_2^{(1)}$ and $\epsilon^2\sigma_2^{(2)}$, which are derived in Eq.(131), respectively. The open circles, the open squares, the Greek crosses and the open triangles represent numerical results of Re$[\sigma^{(1)}]$, Re$[\sigma^{(2)}]$, Re$[\sigma^{(3)}]$ and Re$[\sigma^{(4)}]$, respectively. (b) The solid and the broken lines are $\epsilon\sigma_1^{(3)}$ and $\epsilon\sigma_1^{(4)}$, which are derived in Eq.(117), respectively. Here, $\sigma_1^{(1)} = \sigma_1^{(2)} = 0$. The open circles, the open squares, the Greek crosses and the open triangles represent numerical results of Im$[\sigma^{(1)}]$, Im$[\sigma^{(2)}]$, Im$[\sigma^{(3)}]$ and Im$[\sigma^{(4)}]$, respectively. Here, the mean area fraction $\nu_0 = 0.3$.

If we multiply $\tilde{\varphi}_0^{(2)}$ to Eq.(136), we find

$$\tilde{\varphi}_0^{(2)}\mathcal{L}_2\psi_1 + C\tilde{\varphi}_0^{(2)}\mathcal{L}_2\varphi_0^{(2)} + \tilde{\varphi}_0^{(2)}\mathcal{L}_3\varphi_0^{(1)} = \sigma_2^{(1)}\left(\tilde{\varphi}_0^{(2)}\psi_1 + C\right) . \tag{137}$$

Since $\tilde{\varphi}_0^{(2)}\mathcal{L}_2\varphi_0^{(2)} = \sigma_2^{(2)}$ and $\tilde{\varphi}_0^{(2)}\mathcal{L}_3\varphi_0^{(1)} = \tilde{\varphi}_0^{(2)}\psi_1 = 0$, the constant C is given by

$$C = \frac{\tilde{\varphi}_0^{(2)}\mathcal{L}_2\psi_1}{\sigma_2^{(1)} - \sigma_2^{(2)}} = \frac{2\sqrt{2}q\nu_0\theta_0 p_0\kappa_0}{(\sigma_2^{(2)} - \sigma_2^{(1)})J^3} . \tag{138}$$

On the other hand, if we multiply $\tilde{\varphi}_0^{(1)}$ to Eq.(136), we find

$$\sigma_3^{(1)} = 0 . \tag{139}$$

In the same way, we can find the corresponding left vector $\tilde{\varphi}_1^{(1)}$ in the form

$$\tilde{\varphi}_1^{(1)} = \tilde{\psi}_1 + \tilde{C}\tilde{\varphi}_0^{(2)} , \tag{140}$$

where $\tilde{\psi}_1$ is defined as

$$\tilde{\psi}_1 \equiv -\sum_{n=3,4}\frac{1}{i\sigma_1^{(n)}}(\tilde{\varphi}_0^{(1)}\mathcal{L}_2\varphi_0^{(n)})\tilde{\varphi}_0^{(n)} = \left(\frac{\theta_0 p_0'}{2\sqrt{2}qJ^2}, 0, 0, \frac{p_0}{2\sqrt{2}qJ^2}\right)^{\mathrm{T}} , \tag{141}$$

and a constant $\tilde{C}$ is given by

$$\tilde{C} = \frac{\tilde{\psi}_1\mathcal{L}_2\varphi_0^{(2)}}{\sigma_2^{(1)} - \sigma_2^{(2)}} = \frac{\sqrt{2}q\theta_0 p_0 p_0'\kappa_0}{(\sigma_2^{(2)} - \sigma_2^{(1)})J^3} . \tag{142}$$

Next, we calculate $\varphi_2^{(1)}$ and the corresponding left vector $\tilde{\varphi}_2^{(1)}$. If we multiply $\varphi_0^{(n)}\tilde{\varphi}_0^{(n)}$ $(n = 3, 4)$ to Eq.(136), we can find $\varphi_2^{(1)}$ in the form

$$\varphi_2^{(1)} = \psi_2 + D\varphi_0^{(1)} , \tag{143}$$

where D is a constant and ψ_2 is defined as

$$\psi_2 \equiv \sum_{n=3,4} \frac{1}{i\sigma_1^{(n)}} \varphi_0^{(n)} \left\{ \tilde{\varphi}_0^{(n)} \left(\sigma_2^{(1)} - \mathcal{L}_2 \right) \varphi_1^{(1)} \right\} = \frac{H}{\sqrt{2}qJ} (0,1,1,0)^{\mathrm{T}} \ . \tag{144}$$

In Eq.(144), we have used the relations

$$\tilde{\varphi}_0^{(n)} \psi_1 = \frac{\theta_0}{4qJ} \ , \tag{145}$$

$$\tilde{\varphi}_0^{(n)} \mathcal{L}_2 \varphi_0^{(2)} = -\frac{2\sqrt{2}q^2\theta_0 p_0 p_0' \kappa_0}{J^2} \ , \tag{146}$$

$$\tilde{\varphi}_0^{(n)} \mathcal{L}_2 \psi_1 = -\frac{2q\theta_0 p_0^2 \kappa_0}{J^3} \ , \tag{147}$$

$$\tilde{\varphi}_0^{(n)} \mathcal{L}_3 \varphi_0^{(1)} = 0 \ , \tag{148}$$

and the constant H is given by

$$H = \frac{\theta_0}{4qJ} \sigma_2^{(1)} + \frac{2\sqrt{2}q^2\theta_0 p_0 p_0' \kappa_0}{J^2} C + \frac{2q\theta_0 p_0^2 \kappa_0}{J^3} \ . \tag{149}$$

In the same way, we can find the corresponding left vector $\tilde{\varphi}_2^{(1)}$ in the form

$$\tilde{\varphi}_2^{(1)} = \tilde{\psi}_2 + \tilde{D} \tilde{\varphi}_0^{(1)} \ , \tag{150}$$

where $\tilde{D}$ is a constant and $\tilde{\psi}_2$ is defined as

$$\tilde{\psi}_2 \equiv \sum_{n=3,4} \frac{1}{i\sigma_1^{(n)}} \left\{ \tilde{\varphi}_1^{(1)} \left(\sigma_2^{(1)} - \mathcal{L}_2 \right) \varphi_0^{(n)} \right\} \tilde{\varphi}_0^{(n)} = -\frac{\theta_0 \tilde{H}}{\sqrt{2}qJ} (0,1,1,0)^{\mathrm{T}} \tag{151}$$

with the constant

$$\tilde{H} = \frac{1}{4qJ} \sigma_2^{(1)} + \frac{4\sqrt{2}q^2\nu_0 p_0 \kappa_0}{J^2} \tilde{C} + \frac{2qp_0^2\kappa_0}{J^3} \ . \tag{152}$$

Because the eigenvector $\varphi_q^{(1)}$ defined in Eq.(128) is orthogonal and normalized, we can find that the constants D and $\tilde{D}$ are given by

$$D = -\frac{\theta_0}{8J^2} - \frac{C\tilde{C}}{J} \ , \tag{153}$$

$$\tilde{D} = \left(\frac{1}{J} - 1 \right) C\tilde{C} \ . \tag{154}$$

We find the eigenvector and the corresponding left eigenvector of Eq.(109) up to the second order of ϵ as

$$\begin{aligned} \varphi_q^{(1)} &= \varphi_0^{(1)} + \epsilon\varphi_1^{(1)} + \epsilon^2\varphi_2^{(1)} \\ &= \begin{pmatrix} 0 \\ \frac{1}{\sqrt{2}} \\ -\frac{1}{\sqrt{2}} \\ 0 \end{pmatrix} + \epsilon \begin{pmatrix} \frac{\nu_0\theta_0}{2\sqrt{2}qJ^2} - \frac{p_0 C}{J} \\ 0 \\ 0 \\ \frac{\theta_0 p_0}{\sqrt{2}qJ^2} + \frac{\theta_0 p_0' C}{J} \end{pmatrix} + \epsilon^2 \begin{pmatrix} 0 \\ \frac{H}{\sqrt{2}qJ} + \frac{D}{\sqrt{2}} \\ \frac{H}{\sqrt{2}qJ} - \frac{D}{\sqrt{2}} \\ 0 \end{pmatrix} \ , \end{aligned} \tag{155}$$

and

$$\begin{aligned} \tilde{\varphi}_q^{(1)} &= \tilde{\varphi}_0^{(1)} + \epsilon\tilde{\varphi}_1^{(1)} + \epsilon^2\tilde{\varphi}_2^{(1)} \\ &= \begin{pmatrix} 0 \\ \frac{1}{\sqrt{2}} \\ -\frac{1}{\sqrt{2}} \\ 0 \end{pmatrix} + \epsilon \begin{pmatrix} \frac{\theta_0 p_0'}{2\sqrt{2}qJ^2} - \frac{2p_0\tilde{C}}{J} \\ 0 \\ 0 \\ \frac{p_0}{2\sqrt{2}qJ^2} + \frac{\nu_0\tilde{C}}{J} \end{pmatrix} + \epsilon^2 \begin{pmatrix} 0 \\ -\frac{\theta_0\tilde{H}}{\sqrt{2}qJ} + \frac{\tilde{D}}{\sqrt{2}} \\ -\frac{\theta_0\tilde{H}}{\sqrt{2}qJ} - \frac{\tilde{D}}{\sqrt{2}} \\ 0 \end{pmatrix} \ , \end{aligned} \tag{156}$$

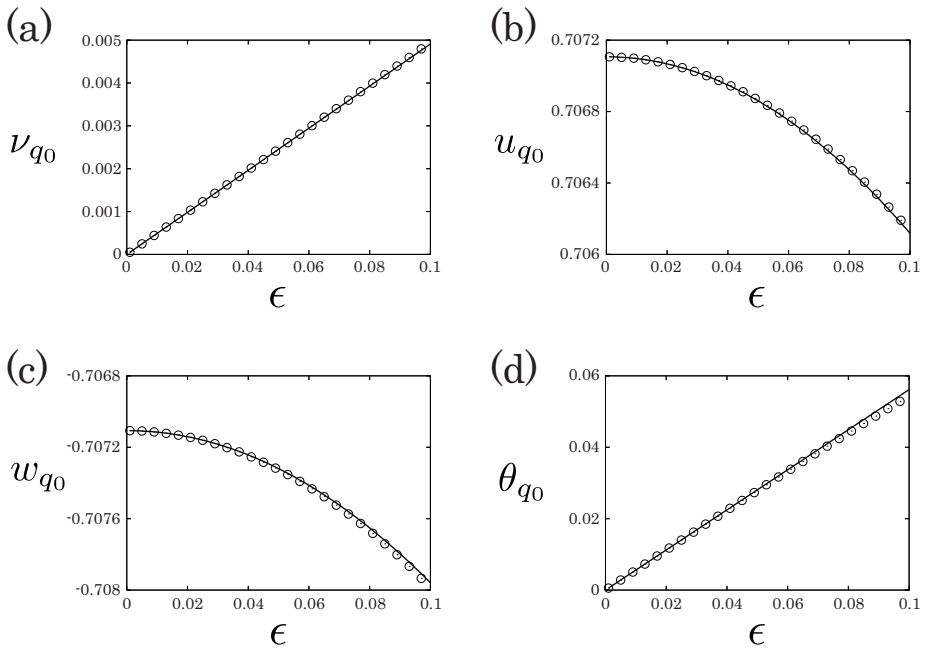

Fig. 8 The results of perturbative calculation Eq.(155) and numerical results of (a)ν_{q_0}, (b)u_{q_0}, (c)w_{q_0} and (d)θ_{q_0}, respectively. The solid lines and the open circles represent the analytic form Eq.(155) and numerical results of Eq.(109), respectively, for the mean area fraction $\nu_0 = 0.3$.

respectively.

Let us compare the results of our perturbative calculation Eq.(155) with results of numerical calculation of $\varphi_q = (\nu_{q_0}, u_{q_0}, w_{q_0}, \theta_{q_0})^{\mathrm{T}}$. In Fig.8, the solid lines and the open circles represent the analytic form Eq.(155) and numerical results of Eq.(109) obtained by LAPACK [68], respectively. From this result, it is confirmed that the perturbative solution of φ_q is correct in the range $0 < \epsilon < 0.1$. We have also confirmed that Eq.(156) well explain the numerical results of $\tilde{\varphi}_q = (\tilde{\nu}_{q_0}, \tilde{u}_{q_0}, \tilde{w}_{q_0}, \tilde{\theta}_{q_0})^{\mathrm{T}}$ in the range $0 < \epsilon < 0.1$.

Finally, we find

$$\mathcal{L}_1\varphi_3^{(1)} + \mathcal{L}_2\varphi_2^{(1)} + \mathcal{L}_3\varphi_1^{(1)} + \mathcal{L}_4\varphi_0^{(1)} = \sigma_4^{(1)}\varphi_0^{(1)} + \sigma_2^{(1)}\varphi_2^{(1)} \ , \tag{157}$$

at $O(\epsilon^4)$ of Eq.(109). If we multiply $\tilde{\varphi}_0^{(1)}$ to Eq.(157), we find

$$\sigma_4^{(1)} = -\frac{H}{2qJ} \ . \tag{158}$$

Thus, from Eqs.(131), (138), (149) and (158), the eigenvalue $\sigma^{(1)}$ up to the fourth order of ϵ is written as a function of q:

$$\begin{aligned} \sigma^{(1)}(q) &= \epsilon^2\sigma_2^{(1)}(q) + \epsilon^4\sigma_4^{(1)}(q) \\ &= \epsilon^2\left(\frac{1}{2} - \epsilon^2 c\right) - \eta_0\epsilon^2 q^2 - \frac{\epsilon^4\theta_0}{16J^2q^2} - \frac{\epsilon^4 a}{bJ^2(bq^2 - J^2)} \ , \end{aligned} \tag{159}$$

where we have introduced the constants

$$a = 8\nu_0\theta_0^2 p_0^2 p_0'\kappa_0^2 \ , \tag{160}$$

$$b = 2(\eta_0 J^2 - 4\nu_0\theta_0 p_0'\kappa_0) \ , \tag{161}$$

$$c = \frac{\theta_0\eta_0(4\kappa_0 - \eta_0)}{8\left\{2\eta_0 p_0^2 - \nu_0\theta_0 p_0'(4\kappa_0 - \eta_0)\right\}} \ . \tag{162}$$

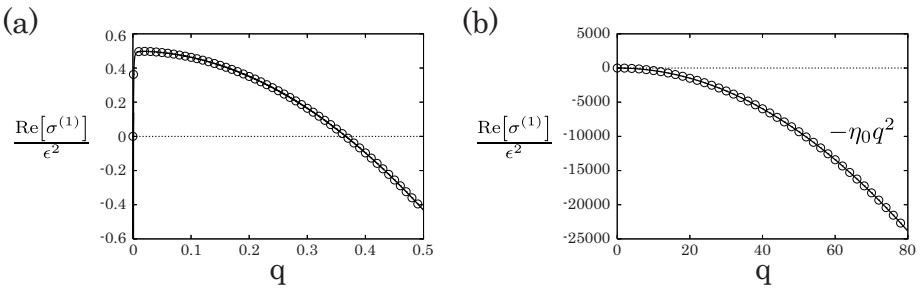

Fig. 9 (a) $\mathrm{Re}[\sigma^{(1)}]/\epsilon^2$ in the vicinity of $q = 0$, where the solid line and the open circles represent the analytic form Eq.(159) and numerical results for $\epsilon = 0.01$ and $\nu_0 = 0.3$, respectively. (b) $\mathrm{Re}[\sigma^{(1)}]/\epsilon^2$ in the short wave length $q \gg 1$, where the solid line and the open circles represent $-\eta_0 q^2$ and numerical results for $\epsilon = 0.01$ and $\nu_0 = 0.3$, respectively.

Let us compare the result Eq.(159) with numerical calculation. In Fig.9, the solid lines and the open circles represent $\mathrm{Re}[\sigma^{(1)}]/\epsilon^2$ given by Eq.(159) and the numerical results for $\epsilon = 0.01$, respectively. From this result, the behavior of $\sigma^{(1)}$ is well reproduced by Eq.(159).

References

1. S. Luding, Nonlinearity **22**, R101 (2009)
2. T. Pöschel, S. Luding (eds.), *Granular Gases* (Springer-Verlag, Berlin, 2001)
3. N.V. Brilliantov, T. Pöschel, *Kinetic Theory of Granular Gases* (Oxford University Press, Oxford, 2004)
4. I. Goldhirsch, Annu. Rev. Fluid Mech. **35**, 267 (2003)
5. Y. Forterre, O. Pouliquen, Annu. Rev. Fluid Mech. **40**, 1 (2008)
6. H. Jeager, S. Nagel, R. Behringer, Rev. Mod. Phys. **68**, 1259 (1996)
7. S. Chong, M. Otsuki, H. Hayakawa, S. Luding, Phys. Rev. E **81**, 041130 (2010)
8. O. Pouliquen, Phys. Fluids **11**, 542 (1999)
9. N. Sela, I. Goldhirsch, S.H. Noskowicz, Phys. Fluids **8**, 2337 (1996)
10. A. Santos, V. Garzó, J.W. Dufty, Phys. Rev. E **69**, 061303 (2004)
11. M.L. Tan, I. Goldhirsch, Phys. Fluids **9**, 856 (1997)
12. K. Saitoh, H. Hayakawa, Phys. Rev. E **75**, 021302 (2007)
13. V. Kumaran, Phys. Rev. Lett. **96**, 258002 (2006)
14. V. Kumaran, Phys. Rev. E **79**, 011301 (2009)
15. V. Kumaran, Phys. Rev. E **79**, 011302 (2009)
16. A. Orpe, A. Kudrolli, Phys. Rev. Lett. **98**, 238001 (2007)
17. A. Orpe, V. Kumaran, K. Reddy, A. Kudrolli, Europhys. Lett. **84**, 64003 (2008)
18. C. Rycroft, A. Orpe, A. Kudrolli, Phys. Rev. E **80**, 031305 (2009)
19. M. Otsuki, H. Hayakawa, Eur. Phys. J. Special Topics **179**, 179 (2009)
20. M. Otsuki, H. Hayakawa, J. Stat. Mech: Theor. Exp. p. L08003 (2009)
21. M. Otsuki, H. Hayakawa, Phys. Rev. E **79**, 021502 (2009)
22. M.Y. Louge, Phys. Fluids **6**, 2253 (1994)
23. M.Y. Louge, Phys. Rev. E **67**, 061303 (2003)
24. H. Xu, A.P. Reeves, M.Y. Louge, Rev. Sci. Instrum. **75**, 811 (2004)
25. H. Xu, M.Y. Louge, A.P. Reeves, Continuum Mech. Thermodyn. **15**, 321 (2003)
26. E. Khain, Phys. Rev. E **75**, 051310 (2007)
27. E. Khain, Eur. Phys. Lett. **87**, 14001 (2009)
28. G. Midi, Eur. Phys. J. E **14**, 341 (2004)
29. F. da Cruz, S. Eman, M. Prochnow, J. Roux, F. Chevoir, Phys. Rev. E **72**, 021309 (2005)
30. T. Hatano, Phys. Rev. E **75**, 060301(R) (2007)
31. M. van Hecke, J. Phys. Condens. Matter **22**, 033101 (2010)
32. T. Hatano, M. Otsuki, S. Sasa, J. Phys. Soc. Jpn. **76**, 023001 (2007)
33. T. Hatano, J. Phys. Soc. Jpn. **77**, 123002 (2008)

34. M. Otsuki, H. Hayakawa, Prog. Theor. Phys. **121**, 647 (2009)
35. M. Otsuki, H. Hayakawa, Phys. Rev. E **80**, 011308 (2009)
36. M. Otsuki, H. Hayakawa, S. Luding, Prog. Theor. Phys. Suppl. **184**, 110 (2010)
37. C.K.K. Lun, J. Fluid Mech. **233**, 539 (1991)
38. J.J. Brey, J.W. Dufty, C.S. Kim, A. Santos, Phys. Rev. E **58**, 4638 (1998)
39. V. Garzó, J.W. Dufty, Phys. Rev. E **59**, 5895 (1998)
40. J.F. Lutsko, Phys. Rev. E **70**, 061101 (2004)
41. J.F. Lutsko, Phys. Rev. E **72**, 021306 (2005)
42. J.F. Lutsko, Phys. Rev. E **73**, 021302 (2006)
43. J.T. Jenkins, M.W. Richman, Phys. Fluids **28**, 3485 (1985)
44. J.T. Jenkins, M.W. Richman, Arch. Ration. Mech. Anal. **87**, 355 (1985)
45. M. Alam, P.R. Nott, J. Fluid Mech. **377**, 99 (1998)
46. P.J. Schmid, H.K. Kytömaa, J. Fluid Mech. **264**, 255 (1994)
47. C.H. Wang, R. Jackson, S. Sundaresan, J. Fluid Mech. **308**, 31 (1996)
48. M. Otsuki, H. Hayakawa, arXiv:1006.3597 (2010)
49. P. Shukla, M. Alam, Phys. Rev. Lett. **103**, 068001 (2009)
50. P. Shukla, M. Alam, J. Fluid Mech. in press (2010)
51. J.T. Stuart, J. Fluid Mech. **9**, 353 (1960)
52. K. Stewartson, J.T. Stuart, J. Fluid Mech. **48**, 529 (1971)
53. W.C. Reynolds, M.C. Potter, J. Fluid Mech. **27**, 465 (1967)
54. A.C. Newell, J.A. Whitehead, J. Fluid Mech. **38**, 279 (1969)
55. Y. Kuramoto, *Chemical Oscillations, Waves and Turbulence* (Springer, Berlin, 1984)
56. I.S. Aranson, L. Kramer, Rev. Mod. Phys. **74**, 99 (2002)
57. M. Cross, P. Hohenberg, Rev. Mod. Phys. **65**, 851 (1993)
58. A.W. Lees, S.F. Edwards, J. Phys. C **5**, 1921 (1972)
59. J. Jenkins, C. Zhang, Phys. Fluids **14**, 1228 (2002)
60. D. Yoon, J. Jenkins, Phys. Fluids **17**, 083301 (2005)
61. L. Verlet, D. Levesque, Mol. Phys. **46**, 969 (1982)
62. D. Henderson, Mol. Phys. **34**, 301 (1977)
63. D. Henderson, Mol. Phys. **30**, 971 (1975)
64. N. Carnahan, K. Starling, J. Chem. Phys. **51**, 635 (1969)
65. O.M. Phillips, Ann. Rev. Fluid Mech. **1**, 245 (1969)
66. G.D. Chagelishvili, T.S. Hristov, R.G. Chanishvili, J.G. Lominadze, Phys. Rev. E **47**, 366 (1993)
67. G.D. Chagelishvili, A.D. Rogava, I.N. Segal, Phys. Rev. E **50**, R4283 (1994)
68. E. Anderson, Z. Bai, C. Bischof, S. Blackford, J. Demmel, J. Dongarra, J.D. Croz, A. Greenbaum, S. Hammarling, A. McKenney, D. Sorensen, *LAPACK Users' Guide*, 3rd edn. (Society for Industrial and Applied Mathematics, Philadelphia, PA, 1999)
69. M.C. Cross, P.G. Daniels, P.C. Hohenberg, E.D. Siggia, J. Fluid Mech. **127**, 155 (1983)
70. W. van Saarloos, Phys. Rev. A **39**, 6367 (1989)
71. T.S. Komatsu, H. Hayakawa, Phys. Lett. A **183**, 56 (1993)